2 mic

X-550-71-504
PREPRINT

NASA TM X- 70700

THE GRAVIMETRIC GEODESY INVESTIGATION

JOSEPH W. SIRY

AUGUST 1971

GSFC
GODDARD SPACE FLIGHT CENTER
GREENBELT, MARYLAND

X-550-71-504
Preprint

THE GRAVIMETRIC GEODESY INVESTIGATION

Joseph W. Siry

August 1971

Goddard Space Flight Center
Greenbelt, Maryland

THE GRAVIMETRIC GEODESY INVESTIGATION

by

Joseph W. Siry

ABSTRACT

The Gravimetric Geodesy Investigation will utilize altimeter and satellite-to-satellite tracking data from GEOS-C, ATS-F, and other spacecraft as appropriate to improve our knowledge of the earth's gravitational field. This investigation is interrelated with the study of oceanographic phenomena such as those associated with tides and currents, hence the latter are considered together with gravitational effects in preparing for the analysis of the data. The oceanographic effects, each of the order of a meter or two in amplitude and with still smaller uncertainties, will not seriously hamper the initial altimeter gravimetric studies at the five meter level. Laser and satellite-to-satellite tracking data, when combined with the altimeter results, should provide the basis for such studies over wide areas of the ocean surface. Laser and conventional geodetic tracking data from ISAGEX and succeeding campaigns will provide a valuable framework for these analyses.

The use of submeter altimeter capabilities together with the decimeter laser systems being developed under the NASA Earth Physics Program will open up the possibility of investigating tides and current meanders in areas such as the Goddard-Bermuda-Bay of Fundy traingle, for example.

Satellite-to-satellite tracking between GEOS-C and ATS-F and also between ATS and the Nimbus, Atmosphere Explorer and SAS-C spacecraft will make possible advances in the range from half to one order of magnitude in connection with the spatial resolution of gravitational features. Improvements of the order of perhaps a factor of two in acceleration resolution will also be looked for.

CONTENTS

THE GRAVIMETRIC GEODESY INVESTIGATION

I. INTRODUCTION

The principal objective of the Gravimetric Geodesy Investigation is to build upon the achievements of the National Geodetic Satellite Program (NGSP) by improving the knowledge of the earth's gravitational field. The NGSP goal is to determine the gravitational field to five parts in a hundred million. It is anticipated that it will be reached by about 1974. This goal includes, specifically, the determination of spherical harmonic coefficients of the geopotential through the fifteenth degree and order with an accuracy such that they contributed no more than 3 milligals root mean square error to the determination of mean anomalies at the Earth's surface in regions which are 12 degrees in latitude by 12 degrees in longitude. (Cf. Reference 1.)

The first goal of the Gravimetric Geodesy Investigation is to utilize the new types of data to be provided by the altimeter and the GEOS-C/ATS-F satellite-to-satellite tracking system to improve the spatial resolution of the gravity field representation over large regions of the earth by a factor of two with comparable or better accuracy, i.e., to determine parameters associated with anomalies in six degree squares with accuracies corresponding to 1 to 3 milligals. The longer range goal is to achieve still another factor of two in resolution and an increase of one to two orders of magnitude in accuracy over the whole earth. (Refs. 2-4.)

The objectives of the investigation will accordingly include the analysis and evaluation of the altimeter and the satellite-to-satellite tracking systems as geodetic instruments. One of the primary aspects of the altimeter calibration problem is the determination of the satellite position, and one of the principal systems which will be used for this purpose is the satellite-to-satellite tracking system. Hence the gravimetric investigation and the satellite-to-satellite tracking and orbit determination investigation are inter-related.

The actual positions of the sea surfaces are affected by a number of oceanographic factors including, in addition to the geoid, the tides, the general circulation, currents and their meanders, sea-state, winds, storm surges and tsunamis. Therefore, in order to conduct the gravimetric investigation properly, it is necessary to represent these oceanographic effects on the sea surface heights appropriately. As in the case of the gravitational field, these representations will come initially from our pre-GEOS information. They will be improved through the analysis of the GEOS-C altimeter data. Thus, the gravimetric and oceanographic investigations are also interrelated. This point is discussed further later.

The phase of the gravimetric investigation, per se, to be conducted before the launching of GEOS-C will involve the use of the additional satellite tracking data including especially the laser data which will become available in the intervening years. This aspect of the investigation will involve the simultaneous

determination of gravimetric quantities and other environmental parameters which contribute to the observational residuals. The aims of this part of the investigation will accordingly include the determination of tracking station locations, quantities such as the Earth's mass and radius, and coefficients representing atmospheric drag and radiation pressure effects. Consideration is being given, too, to the possibility of equipping other spacecraft with the capability for satellite-to-satellite tracking through ATS-F. The potential contributions of such capabilities to the Gravimetric Geodesy Investigation is discussed.

II. EXPLOITATION OF EXISTING DATA IN PREPARATION FOR THE ANALYSIS OF ALTIMETER AND SATELLITE-TO-SATELLITE TRACKING DATA FROM GEOS-C

A. General Considerations

The basic strategy of the investigation is to derive the greatest benefit from the altimeter and satellite-to-satellite tracking data from GEOS-C by analyzing it together with all of the related data which can contribute to the determination of the Earth's gravitational field. The determination of the characteristics of the gravitational field will be based upon the existing stores of geodetic data as well as the additional observational material which will become available in time for use in the analyses of the new types of data to be furnished by GEOS-C. The fundamental body of data upon which our current knowledge of the gravitational field is based consists of approximately a hundred thousand precisely reduced optical observations of some two dozen satellites, a substantial number of

Doppler measures, some range and range rate data, the beginnings of a supply of laser range measurements, as well as the gravimetric and survey results of classical geodesy. It is anticipated that, by the time the analysis of the new data types from GEOS-C commences, this store will be enriched through the addition of considerable numbers of laser observations obtained in programs such as the ISAGEX campaign, and Earth Physics studies such as the polar motion and UTI and fault motion experiments

It is contemplated that the interpretation of these collections of data will involve general determinations of the gravitational field, resonance determinations of geopotential coefficients, and studies involving representations in terms of mass anomalies.

Recent activity in the field of geopotential analysis at several institutions including Goddard is indicated in Tables I and II and discussed in references 28 and 29 which include bibliographies. Results of comparisons of some of the geopotential models listed in Tables I and II are indicated in Table III and in Figure 1. These findings give some idea of the effective accuracies associated with some of the models. Improvements obtained by the modeling of resonant terms are also seen in Table III.

The best published determination of the geopotential which is currently available is the one included in the Smithsonian Astrophysical Observatory 1969 (II) Standard Earth (18). This result was obtained through the use of a general

Table I

General Determinations of Geopotential Coefficients

Author or Designation	Year	Reference Number	Basis			Field Characteristics	
			Satellite Data		Other Information		
			Number of Satellites	Tracking Systems		Last term in Complete Portion	Number of Coefficients
1. NWL 5E-6	1965	1	3	Doppler		7, 6	64
2. APL 3.5	1965	2	5	Doppler		8, 8	84
3. SAO M-1	1966	3	16	Optical		8, 8	122
4. Kaula K-8	1966	4	12	Optical, Doppler		7, 5	99
5. Kaula C	1966	4			Determinations 1-4	7, 2	
6. Rapp	1967	5	16	Optical	Gravimetry	14, 14	219
7. Köhnlein	1967	6	16	Optical	Gravimetry	15, 15	250
8. Kaula UCLA	1967	7	9	Optical, Doppler	Gravimetry	8, 8	
9. Rapp	1968	8	16	Optical	Gravimetry	14, 14	
10. SAO COSPAR	1969	9	24	Optical, Range, Range Rate		14, 14	280
11. SAO B6.1	1969	10	24	Optical, Range, Range Rate		16, 16	
12. SAO B 13.1	1969	11	24	Optical, Range, Range Rate	Gravimetry	16, 16	314
13. SAO SF	1969	12	24	Optical, Range, Range Rate	Gravimetry	16, 16	316
14. GSFC 1.70 C	1970	13			Determinations 1-9, 11, 12	15, 15	249
15. SAO 69 (II)	1970	14	21	Optical, Range, Range Rate	Gravimetry	16, 16	316

Table II

Resonance Determinations of Geopotential Coefficients

Author or Designation	Year	Reference Number	Basis		Field Characteristics
			Numbers and Types Satellites	Reference Coefficients	Coefficients Determined
1. Wagner	1967	19	3 24-hour		(2,2), (3,1), (3,3)
2. Gaposchkin and Veis	1967	20	3 12th order	SAO M-1	(13,12), (14,12), (15,12)
3. Murphy and Victor	1967	21	2 12-hour		(2,2), (4,4)
4. Yionoulis	1968	22	3 13th order		(13,13), (15,13), (17,13)
5. Wagner	1968	23	2 12-hour		(3,2), (4,4)
6. Murphy and Cole	1968	24	1 12th order		(14,12), (15,12)
7. Wagner	1968	25	3 24-hour 2 12-hour		(2,2), (3,1), (3,2) (3,3), (4,4)
8. Douglas and Marsh	1969	26	1 13th Order	Yionoulis, 1968	(14,13)
9. Wagner	1969	27	4 24-hour 4 12-hour	SAO B13.1	(2,2), (3,2), (3,3), (4,4)

TABLE III

Satellite Position Differences Associated with Various Gravity Models

SAO M-1 (modified*) vs.	Position (meters)							
	GEOS I				GEOS II			
	Radial	Cross Track	Along Track	Total	Radial	Cross Track	Along Track	Total
SAO M-1 (unmodified)	30.0	17.1	286.4	288.5	22.3	10.3	232.2	234.2
SAO COSPAR (no. 11th)	8.9	12.8	29.5	33.4	24.7	18.2	92.8	97.8
SAO 1969	8.3	13.5	26.9	31.2	16.6	19.3	59.2	64.4
Köhnlein	16.4	16.1	213.0	214.2	20.1	16.9	129.1	131.7
Köhnlein (modified)	9.2	10.9	28.0	31.4	11.8	15.1	41.9	46.1
Rapp	48.3	29.5	129.4	141.2	38.8	37.7	157.6	166.6
Rapp (modified)	46.4	33.2	99.9	115.0	36.2	39.1	84.8	100.1
APL 3.5	46.1	46.8	175.7	187.1	71.8	55.2	674.3	680.4
APL 3.5 (modified)	42.5	41.6	90.1	107.9	34.7	45.4	88.1	105.2
NWL 5E-6	16.3	16.6	204.0	205.3	46.4	80.9	374.6	386.1
NWL 5E-6 (modified)	16.7	12.9	49.1	53.4	26.3	80.0	82.9	118.2
Kaula	32.5	42.2	114.1	125.9	47.6	43.5	232.8	241.4
Kaula (modified)	32.1	42.5	110.2	122.4	48.7	42.0	140.5	154.6

*Gaposchkin & Veis (1967) 12th order terms for GEOS-I and Yionoulis (1968) and Douglas & Marsh (1968) 13th order terms for GEOS-II.

perturbation theory of satellite motion. Geopotential coefficients and tracking station coordinates were adjusted to provide a best representation of observational data from twenty-one satellites and from gravimetric analyses.

B. Tesseral Harmonic Coefficients

The Gravimetric Geodesy Investigation proceeds along several lines of attack. The immediate aim of one of the approaches is to derive a new general determination of the geopotential using a body of observational material which is more extensive than the one upon which the SAO 1969 (II) Standard Earth model is based. The additions include a large body of material developed in the analysis of synchronous and semisynchronous satellites, i.e., those having

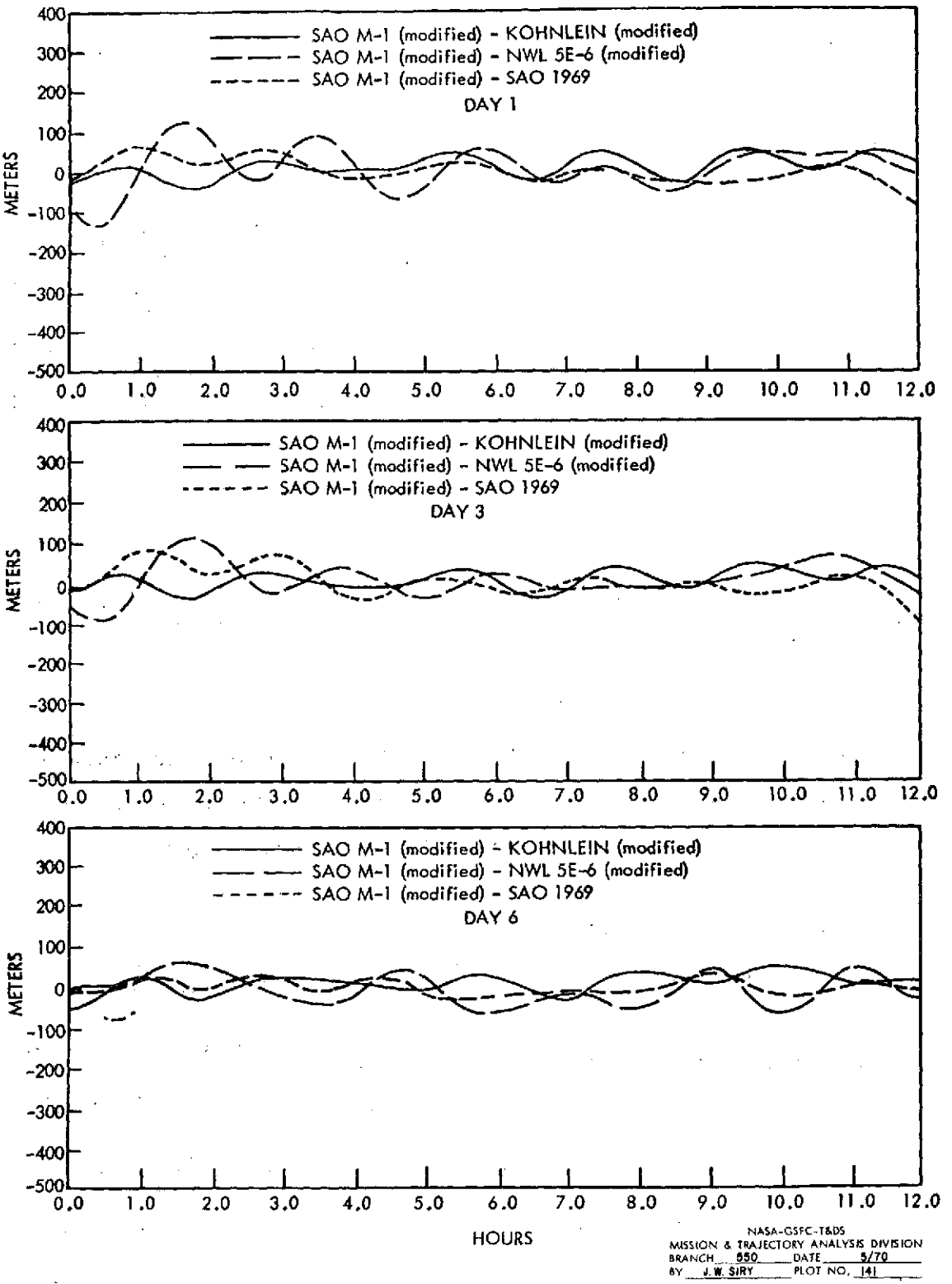

Figure 1. Along Track Position Differences GEOS-I July 11-16, 1966

periods near a day and half a day, respectively. This effort has been carried on over a number of years at Goddard and represents the principal contribution to the analysis of the motions of these types of satellites and of the corresponding features of the earth's gravitational field.

Some of the results obtained by Wagner, Murphy and Victor are contained in references 19, 21, 23-25, and 27 summarized in references 28 and 29 and indicated in Figures 2 through 5 and Tables IV and V.

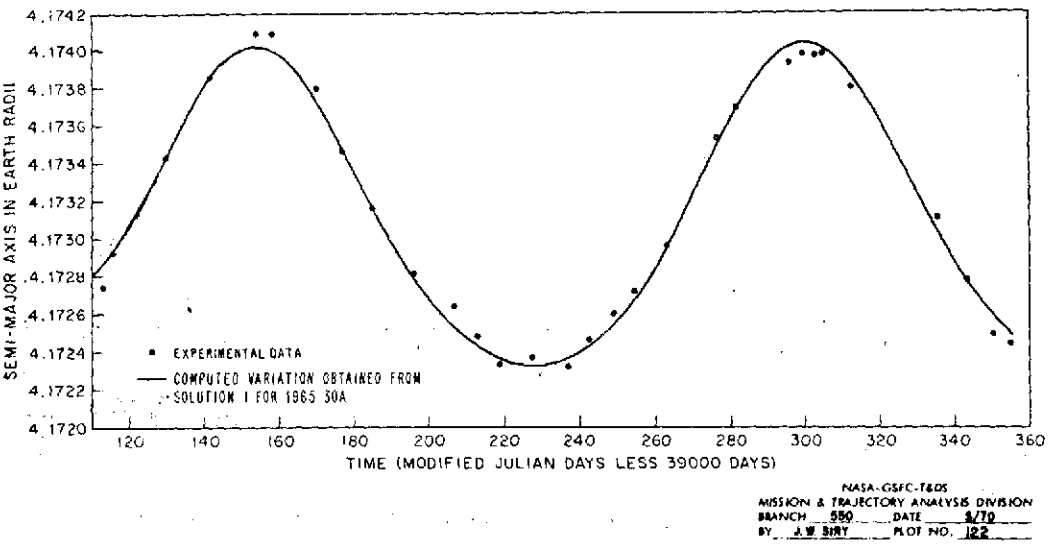

Figure 2. Semi-Major Axis of 1965 30A [Molniya 1] vs. Time.

The possibilities for obtaining an improved geopotential solution through the more extensive use of synchronous and semi-synchronous satellite data are indicated in Table VI where it is seen that relatively small changes in the coefficients result in a significant improvement in the fits to the orbital data. An improvement of about a factor of five is obtained in residuals for synchronous

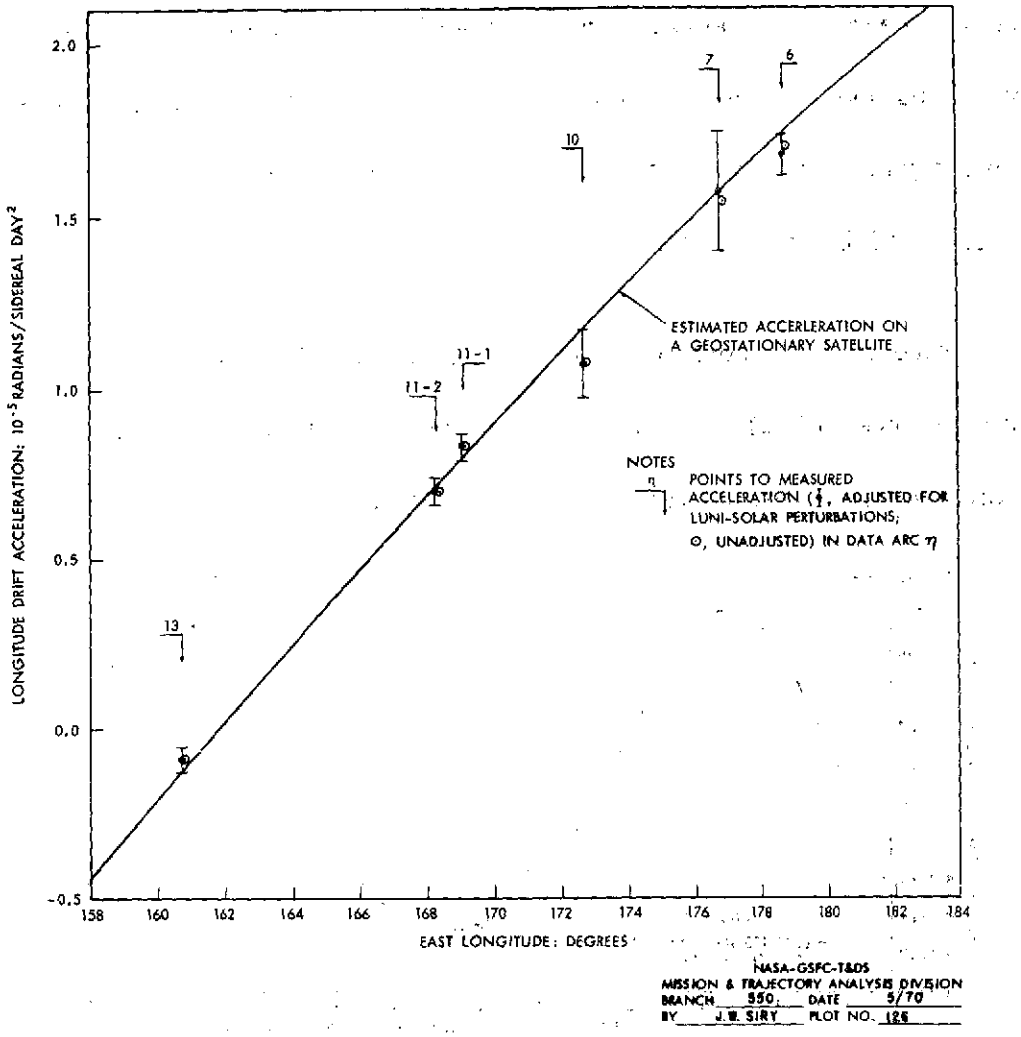

Figure 3. Drift Acceleration in Syncom 3 Arcs 6, 7, 10, 11 and 13.

and semisynchronous satellites by solving for four pairs of tesseral harmonic coefficients in the context of a recent SAO general field. Improved values for low order harmonics which represent these features, and for the general field as a whole, are accordingly expected to result from the inclusion of these added data. The new material in this solution will also reflect some additional optical, range and range rate, and laser observations of the types of satellites the SAO 1969 (II) solution is based on, i.e., those at medium altitudes.

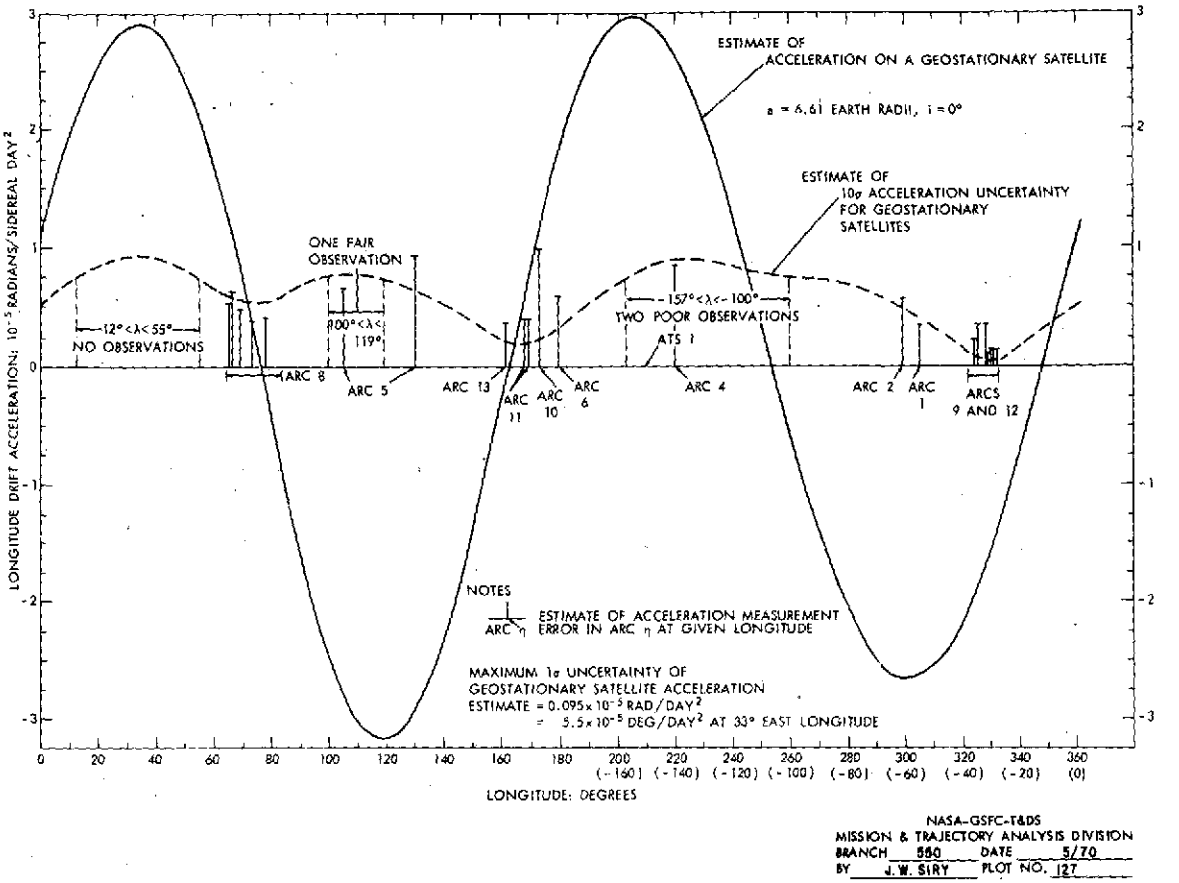

Figure 4. Drift Acceleration and Estimate of Acceleration Uncertainties on 24 Hour Satellites

The present general solution for the geopotential will be carried out by means of a special perturbation theory of satellite motion using a program system described in reference 25. This method is fundamentally different from the one employed by SAO, hence this effort provides a unique opportunity to conduct an independent comparative analysis of the data used in the SAO solution. In addition, increased accuracy should also be more readily achievable by means of the approach employed here.

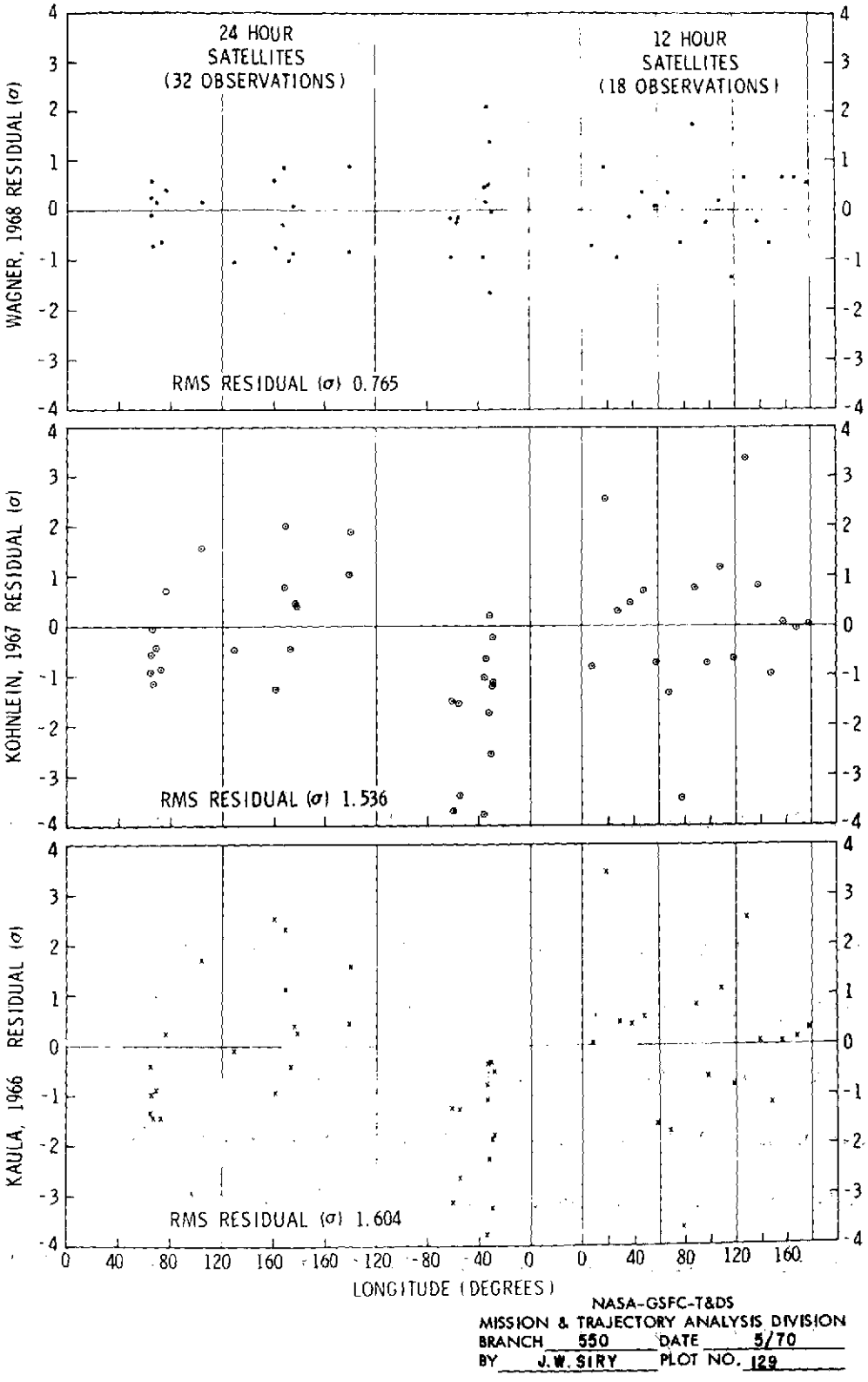

Figure 5. Observation Residuals for 12- and 24-Hour Satellite Accelerations from Recent Geoids.

TABLE IV

Solution for Gravity Coefficients From 24-Hour Satellite Data

SOLUTION (TEST #)	DATA (32 PTS)	$10^7 S^*$ (RAD/DAY^2)	$10^6 C_{22}$	$10^6 S_{22}$	$10^6 C_{31}$	$10^6 S_{31}$	$10^6 C_{33}$	$10^6 S_{33}$	$10^8 C_{44}$	$10^8 S_{44}$
1	UNADJUSTED, UNWEIGHTED	19.8	1.590 ±0.04	-0.970 ±0.04						
2	UNADJUSTED, UNWEIGHTED	5.54	1.578 ±0.011	-0.936 ±0.012			0.051 ±0.009	0.155 ±0.009		
3	UNADJUSTED, WEIGHTED	3.57	1.562 ±0.011	-0.932 ±0.011			0.066 ±0.006	0.168 ±0.007		
4	ADJUSTED, WEIGHTED	2.61	1.558 ±0.012	-0.928 ±0.012			0.064 ±0.007	0.171 ±0.008		
5	UNADJUSTED, WEIGHTED	3.08	1.543 ±0.011	-0.920 ±0.012	-0.57 ±0.83	-1.36 ±0.58	0.027 ±0.013	0.148 ±0.008		
6	ADJUSTED, WEIGHTED	2.49	1.547 ±0.015	-0.913 ±0.014	0.28 ±1.00	-1.47 ±0.74	0.029 ±0.017	0.155 ±0.011		
7	UNADJUSTED, WEIGHTED	3.55	1.551 ±0.013	-0.921 ±0.014			0.064 ±0.010	0.160 ±0.010	-0.29 ±0.87	-1.28 ±0.90
8	ADJUSTED, WEIGHTED	2.71	1.559 ±0.016	-0.927 ±0.018			0.066 ±0.012	0.170 ±0.011	-0.15 ±0.83	0.18 ±1.08
9	UNADJUSTED, WEIGHTED	3.12	1.546 ±0.012	-0.88 ±0.05	1.8 ±3.3	-2.6 ±1.3	0.036 ±0.021	0.133 ±0.018	-1.8 ±2.1	0.23 ±1.4
10	ADJUSTED, WEIGHTED	2.25	1.551 ±0.014	-0.86 ±0.08	3.4 ±3.5	-3.5 ±1.4	0.039 ±0.024	0.127 ±0.021	-3.1 ±2.3	1.1 ±1.7
11	ADJUSTED, WEIGHTED	2.43	1.546 ±0.015	-0.916 ±0.013	0.06 ±0.98	-1.64 ±0.72	0.025 ±0.017	0.154 ±0.011	K66**	(ALSO H_{42})
12	ADJUSTED, WEIGHTED	3.15	1.585 ±0.015	-0.931 ±0.014	K66**		0.087 ±0.008	0.184 ±0.010	K66**	(ALSO H_{42})

NOTES * S = ESTIMATE OF STANDARD ERROR (RMS RESIDUAL) FOR GRAVITY SOLUTION OVER ALL THE DATA.

** COEFFICIENTS FIXED FROM A 1966 DETERMINATION OF KAULA

BEST RESULTS (FROM SOLUTION 6 WITH BOUNDS INCREASED DUE TO LIKELY MODEL ERRORS):

$$10^6 C_{22} = 1.550 \; {}^{+0.035}_{-0.025}, \quad 10^6 S_{22} = -0.915 \pm 0.025$$

$$10^6 C_{31} = 0.3 \; {}^{+2.5}_{-1.6}, \quad 10^6 S_{31} = -1.5 \; {}^{+1.2}_{-1.5}$$

$$10^6 C_{33} = 0.03 \; {}^{+0.06}_{-0.03}, \quad 10^6 S_{33} = 0.155 \pm 0.030$$

$$10^6 J_{22} = 1.80 \pm 0.04, \quad \lambda_{22} = -15.3 \pm 0.6^\circ$$

$$10^6 J_{31} = 1.5 \; {}^{+2.6}_{-1.2}, \quad \lambda_{31} = -.79 \; {}^{+73^\circ}_{-.88^\circ}$$

$$10^6 J_{33} = 0.16 \; {}^{+0.05}_{-0.03}, \quad \lambda_{33} = 26.4 \; {}^{+6.6^\circ}_{-8.3}$$

TABLE V

Resonant Longitude Gravity Coefficients* from Recent Studies

Geoid	C_{22} (10^{-6})	S_{22} (10^{-6})	C_{31} (10^{-6})	S_{31} (10^{-6})	C_{32} (10^{-6})	S_{32} (10^{-6})	C_{33} (10^{-6})	S_{33} (10^{-6})	C_{42} (10^{-6})	S_{42} (10^{-6})	C_{44} (10^{-6})	S_{44} (10^{-6})
Köhnlein	2.38	-1.35	1.71	0.23	0.84	-0.51	0.66	1.43	0.35	0.48	0.04	0.30
Kaula [1966]	2.42	-1.36	1.79	0.18	0.78	0.75	0.57	1.42	0.30	0.60	-0.06	0.32
Wagner	2.40 ± .03	-1.43 ± .03	-0.42	-1.58	0.69 ± .20	-0.53 ± .20	0.16	1.10	0.0	0.0	0.02	0.70

*Fully normalized coefficients.

Table VI

Weighted rms Residuals in Two Combined Arc Solutions

with 12- and 24-Hour Satellites (12 Arcs)

Gravity Field Used	Weighted rms Residual	Strongest Resonant Gravity Coefficients Used (unnormalized): 10^{-6}								Other Resonant Coefficients Used
		2,2		3,2		3,3		4,4		
		C	S	C	S	C	S	C	S	
SAO '69 B13.1	5.90	1.55	-.91	.29	-.22	.111	.180	-.0021	.0075	3,1 4,2 for 24-hour satellites; all through 6,2 8,4 and 10,6 giving .01 of strongest effect for 12-hour satellites
SAO '69 B13.1 corrected	0.99	1.58	-.91	.30	-.21	.097	.198	-.0016	.0075	Same as above

Where appropriate, however, in the case of resonances, for example, use will be made of general perturbation approaches such as those discussed in references 21, 24, 28 and 31.

An example of results of such a determination of resonant harmonic coefficients based on Minitrack data is indicated in Figure 6. Results of this type will also be reflected in the overall general solution.

C. Zonal Harmonic Coefficients

Zonal harmonics have also been determined by means of a general perturbation technique 31-33. It is planned to extend this effort and also to use special perturbations to determine zonal harmonics on the basis of data from some twenty satellites.

Resonances have also been determined by means of a numerical integration approach. Results of this kind are indicated in Figures 7 and 8 in reference 26.

It is anticipated that the progress toward the solution will be sufficient to provide a reasonable basis for the analysis of the data to be generated in connection with Project ISAGEX. The program to determine and refine the general solution for the earth's gravitational field using the constantly increasing supply of data will be continued with the aim of providing a sound foundation for the analysis of the new altimeter and satellite-to-satellite tracking data from GEOS-C.

D. GM and the Radius of the Earth

The best determination of the fundamental gravitational parameter of the earth, its mass, which has been made so far has resulted from work which has proceeded entirely independently of the determination of all the rest of the gravitational quantities. The mass is determined best using data from deep space probes travelling toward and beyond the moon from which the Earth appears more like a gravitational point mass. The higher harmonic coefficients, on the

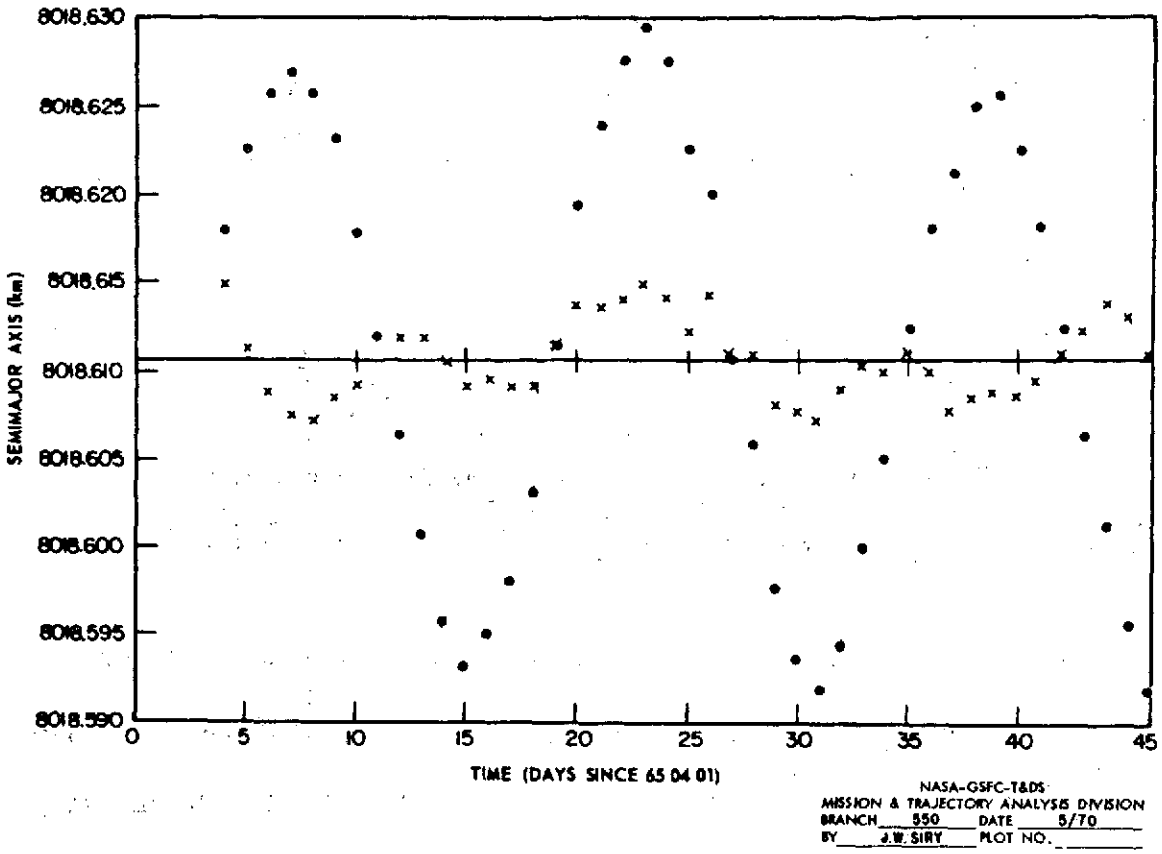

Figure 6. Semimajor Axis of Tiros IX

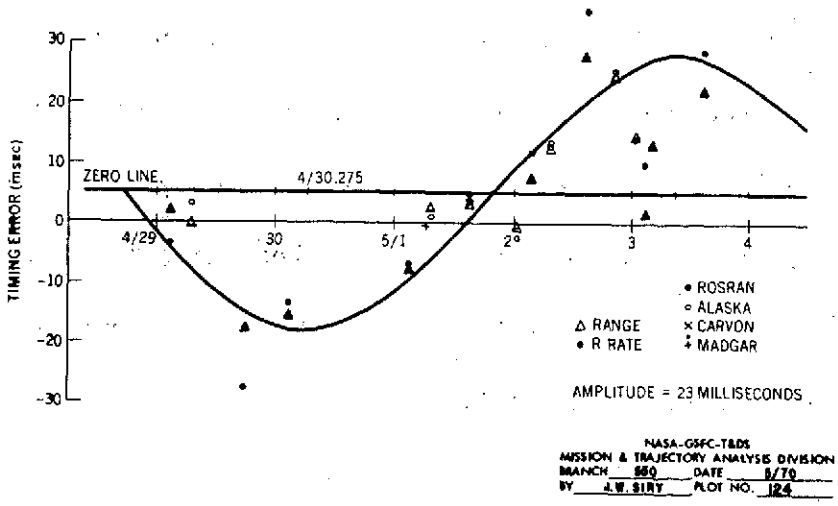

Figure 7. Apparent GEOS-II GRARR Timing Errors SAO M1 Gravity + APL 13th-Order Terms 4/29/68–5/4/68.

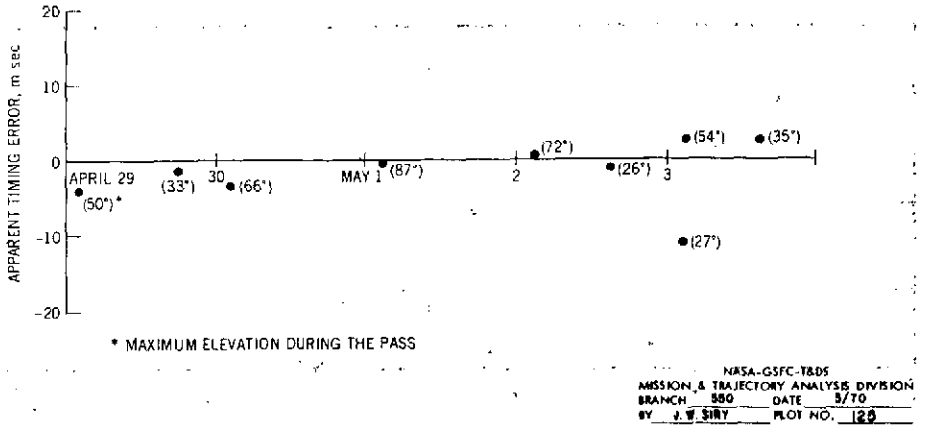

Figure 8. Apparent Rosman Range Timing Errors with SAO M1 Gravity, APL 13th-Order Coefficients and $C_{14,13} = 0.57 \times 10^{-21}$, $S_{14,13} = 6.5 \times 10^{-21}$, 4/29/68 to 5/4/68.

other hand, are best sensed by close earth satellites. Analyses of data from the spacecraft at these two kinds of distances have proceeded separately up to now. This point and some of its implications are discussed in reference (29). The objectives of the Gravimetric Geodesy Investigation also include the determination of the fundamental gravitational quantity, GM, along with the other geopotential parameters and the earth's mean equatorial radius at the same time. Use will be made of accurate range data from spacecraft at several altitudes including some in the one to two thousand kilometer range, some at synchronous heights, as well as others at still greater distances from the earth. Lunar transfer trajectories for which USB tracking data are available are expected to be of special value in this connection.

E. Tracking Station Locations

The determination of geopotential coefficients ultimately will be achieved simultaneously with the determination of tracking station locations. An extensive program for adjustment of tracking station locations has been carried out at Goddard (cf. references 34-37).

In particular, dynamical solutions have been carried out to determine locations of a number of Goddard tracking stations. Some indications of the coverage provided by the thirty thousand observations employed is indicated in Tables 7 and 8 and Figure 9. Results are presented in references 36 and 37.

Table VII

Number of Optical Observations Per Station Used in Dynamical Estimation

STATION		OBSERVATIONS	STATION		OBSERVATIONS
BLOSSOM POINT, MD.	(1021)	650	TANANARIVE, MADAGASCAR	(1043)	339
FT. MYERS, FLA.	(1022)	680	UNIV. OF N. DAKOTA, N. D.	(7034)	548
WOOMERA, AUSTRALIA	(1024)	152	EDINBURG, TEXAS	(7036)	1109
SANTIAGO, CHILE	(1028)	264	COLUMBIA, MO.	(7037)	1540
MOJAVE, CAL.	(1030)	932	BERMUDA	(7039)	448
JOHANNESBURG, UN. OF SO. AFR.	(1031)	623	SAN JUAN, P. R.	(7040)	475
ST. JOHNS, NEWFOUNDLAND	(1032)	179	GREENBELT, MD.	(7043)	158
E. GRAND FORKS, MINN.	(1034)	542	DENVER. COLO.	(7045)	573
WINKFIELD, ENGLAND	(1035)	400	JUPITER, FLA.	(7072)	516
ROSMAN, N. C.	(1037, 1042)	1015	SUDBURY, ONTARIO	(7075)	699
ORRORAL, AUSTRALIA	(1038)	482	KINGSTON, JAMAICA	(7076)	388

Table VIII

GRARR and Laser Arcs Used in Solutions

1968 ARCS

Date	ULASKR			MADGAR			ROSRAN			WALLAS		GODLAS		Optical*
	No. of Obs.			No. of Obs.			No. of Obs.			No. of Obs.		No. of Obs.		
	Range	Range Rate	No. of Passes	Range	Range Rate	No. of Passes	Range	Range Rate	No. of Passes	Range	No. of Passes	Range	No. of Passes	No. of Obs.
4/2-3/68	215	149	3				180	180	3	495	2			374
4/26-27/68	136	84	3				313	313	4	119	1			320
5/7-8/68	172	172	2				102	102	1	480	2			172
5/21-22/68	132	132	2				167	166	4	492	2			351
6/9-10/68	262	262	3				277	277	4					393
6/11-12/68	182	182	3				456	456	5	588	3			828
6/14-15/68	252	252	4				196	197	3					641
6/16-17/68	136	136	2				193	194	3					814
6/21-22/68	271	271	5				269	279	4	422	3			754
6/23-24/68	285	285	5				229	229	4					620
9/24-25/68				111	112	2						69	1	132
9/27-28/68	193	193	3		57	2						38	1	389
10/4-5/68	200	200	3	105	107	2						73	1	286
10/6-7/68	271	271	4	186	189	4								309
10/8-9/68	67	67	1	177	188	4						318	2	507
10/21-22/68	132	132	2									312	2	445
10/23-24/68	202	202	3									437	2	346
TOTALS	3108	2990	48	579	653	14	2376	2393	34	2596	13	1247	9	7821

1969 ARCS

Date	ULASKR*			CARVON			CRMLAS		GODLAS*		Optical*
	No. of Obs.			No. of Obs.			No. of Obs.		No. of Obs.		
	Range	Range Rate	No. of Passes	Range	Range Rate	No. of Passes	Range	No. of Passes	Range	No. of Passes	No. of Obs.
3/2-3/69	127	127	5	158	158	4	99	2	64	1	150
3/5-6/69	124	124	3	92	129	2	227	3	366	4	360
3/11-12/69	99	99	3	232	232	4	190	3	105	2	474
3/13-14/69	150	150	3	314	378	6	199	3	32	1	295
3/17-18/69	196	196	5	232	237	5	214	4	234	3	224
3/29-30/69	92	92	5	170	170	5					225
3/31-4/1/69	164	163	4	192	206	1	101	2			234
4/8-9/69	75	75	2	167	176	4	146	2	94	3	386
4/10-11/69	172	172	5	90	143	2	321	4	73	1	248
4/14-15/69	123	123	3	99	125	3	271	4			230
4/24-25/69	199	199	5	150	179	3	251	2	159	1	452
5/5-6/69	163	163	4	219	280	4	216	4			544
TOTALS	1684	1683	47	2115	2414	43	2235	33	1127	16	3822

*Station coordinates held fixed.

SUMMARY

GRARR	No. of Obs.
range	9862
range rate	10133
number of passes	186
Laser	
range	7205
number of passes	71
Optical	11643
Total	38843

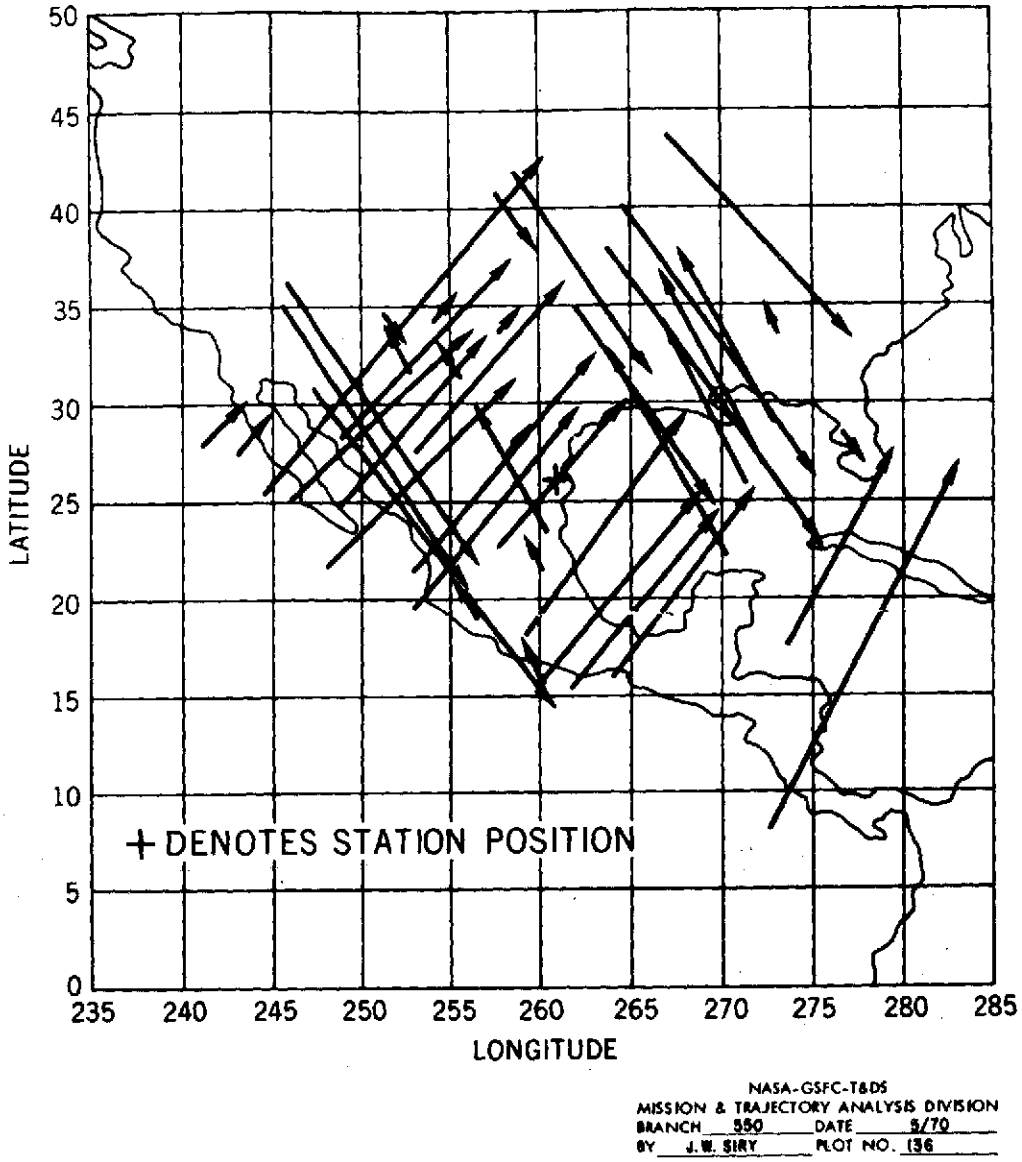

Figure 9. Subsatellite Plot of GEOS-I and GEOS-II Passes, Edinburg, Texas.

III. THE ANALYSIS OF GEOS-C DATA

A. Satellite-to-Satellite Tracking Data

1. The Satellite-to-Satellite Tracking System

The satellite-to-satellite tracking experiment involving a geodetic satellite calls for the tracking of GEOS-C via ATS-F. The quantities to be observed are the range from a ground station through ATS-F to GEOS-C, and the corresponding range difference over a small time interval, which is often referred to as range rate. The use of these data involves the analysis of the motions of both the GEOS-C and the ATS-F spacecraft. It will be possible to make independent measurements of the range and range rate from the ground tracking station to ATS-F using the basic ATS tracking system. It is anticipated that the ATS-F spacecraft will be fitted with laser corner reflectors, and hence that this accurate tracking system can also be used to obtain the range from the ground station to ATS-F. Simultaneous laser observations of ATS from three widely separated points on the Earth's surface can, in fact, permit the determination of the position of ATS-F by entirely geometric means. Such data, together with the continuing analysis of synchronous satellite motions being conducted as part of the Gravimetric Geodesy Investigation, provide a basis for identifying the contributions of ATS effects to the ATS-F/GEOS-C satellite-to-satellite tracking data residuals.

The increase in accuracy resulting from the use of laser tracking of the ATS-F spacecraft by means of a corner reflector array mounted on it is indicated in Figure 10 (38). The circles denote estimates of the errors obtained if

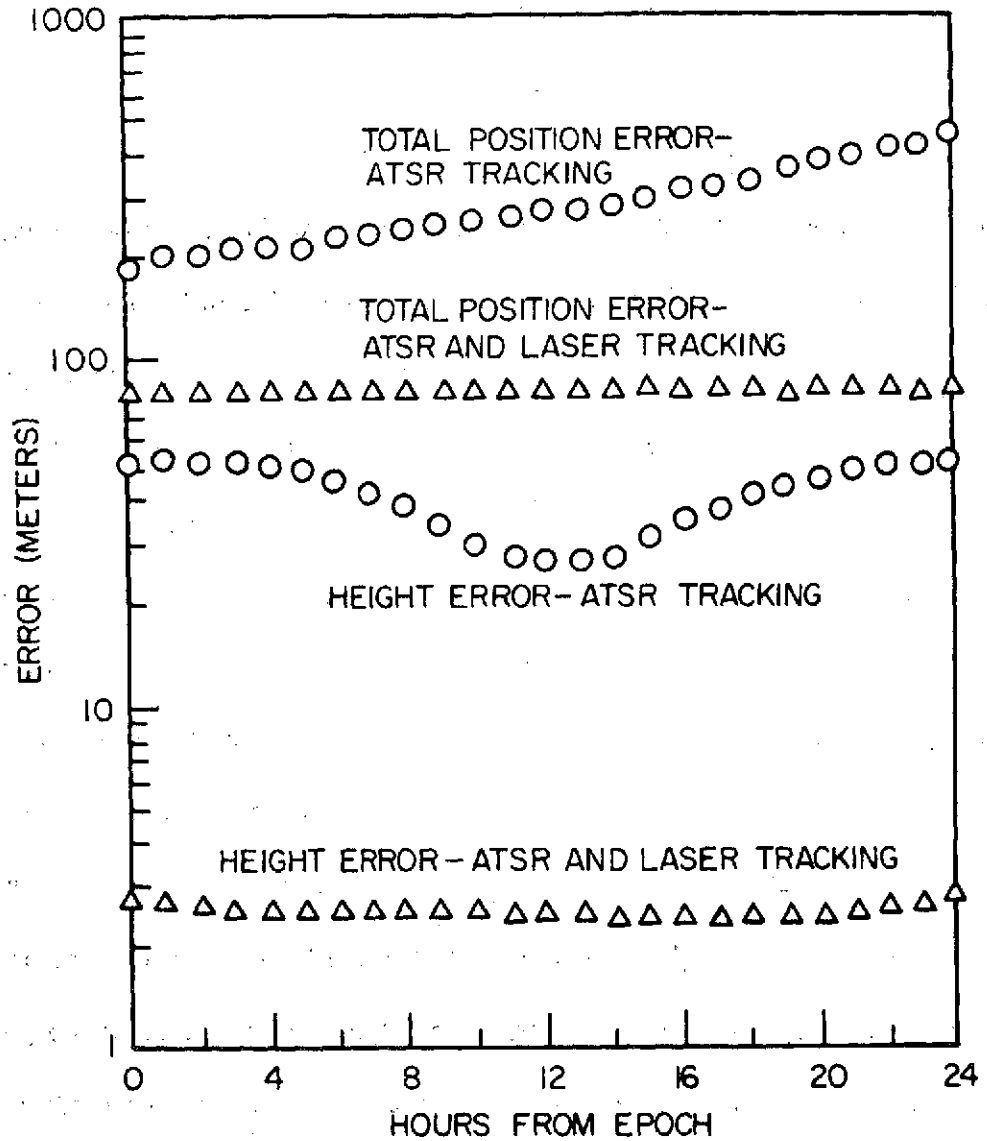

STATIONS: ATSR-NORTH CAROLINA, CALIFORNIA
LASER-MARYLAND, CALIFORNIA, FRENCH GUIANA, CHILE

Lasers: $\sigma = \delta = 0.1$ m
ATSR Range: $\sigma = \delta = 1$ m
ATSR Range Rate $\sigma = 0.035$ cm/s, $\delta = 0$
Cn,m, Sn,m, n,m ≤ 8, 0.25 (SAO - APL)
$\Delta GM/GM$, after adjustment, 0.3 X10

Station:	$\sigma x = \sigma y = \sigma z$ (m)
Goddard	5
Mojave	3
Santiago	8
Kourou	15

Figure 10

the tracking is done only with the ATS electronic range and range rate system. The values assumed for the uncertainties in terms of the noise and bias quantities are also indicated.

The tracking of GEOS-C from ATS-F will be analogous in many ways to the tracking of lunar satellites from stations on the earth. The data from lunar orbiters were originally analyzed in conventional ways in terms of spherical harmonic coefficients. It was realized after a time that many of the lunar satellite range rate tracking data residual anomalies corresponded to mascons or surface density distributions. This interpretational approach is perhaps one of the most striking features of recent research relating to gravitational fields. (Cf. Figure 11.) Both the traditional and the new approaches have been used at Goddard as is pointed out in references 39 and 40.

A satellite experiencing an anomalous acceleration of about four milligals over fifty seconds will undergo a velocity change of a couple of millimeters per second. Increments of this order should be detectable with the aid of satellite-to-satellite tracking equipment now being developed, which will have a resolution of about 0.35 millimeters per second. Such an acceleration could correspond, for example, to a surface gravity anomaly of the order of ten milligals. This point is discussed by Vonbun. A typical case is indicated in Figure 12 which is presented in reference 41.

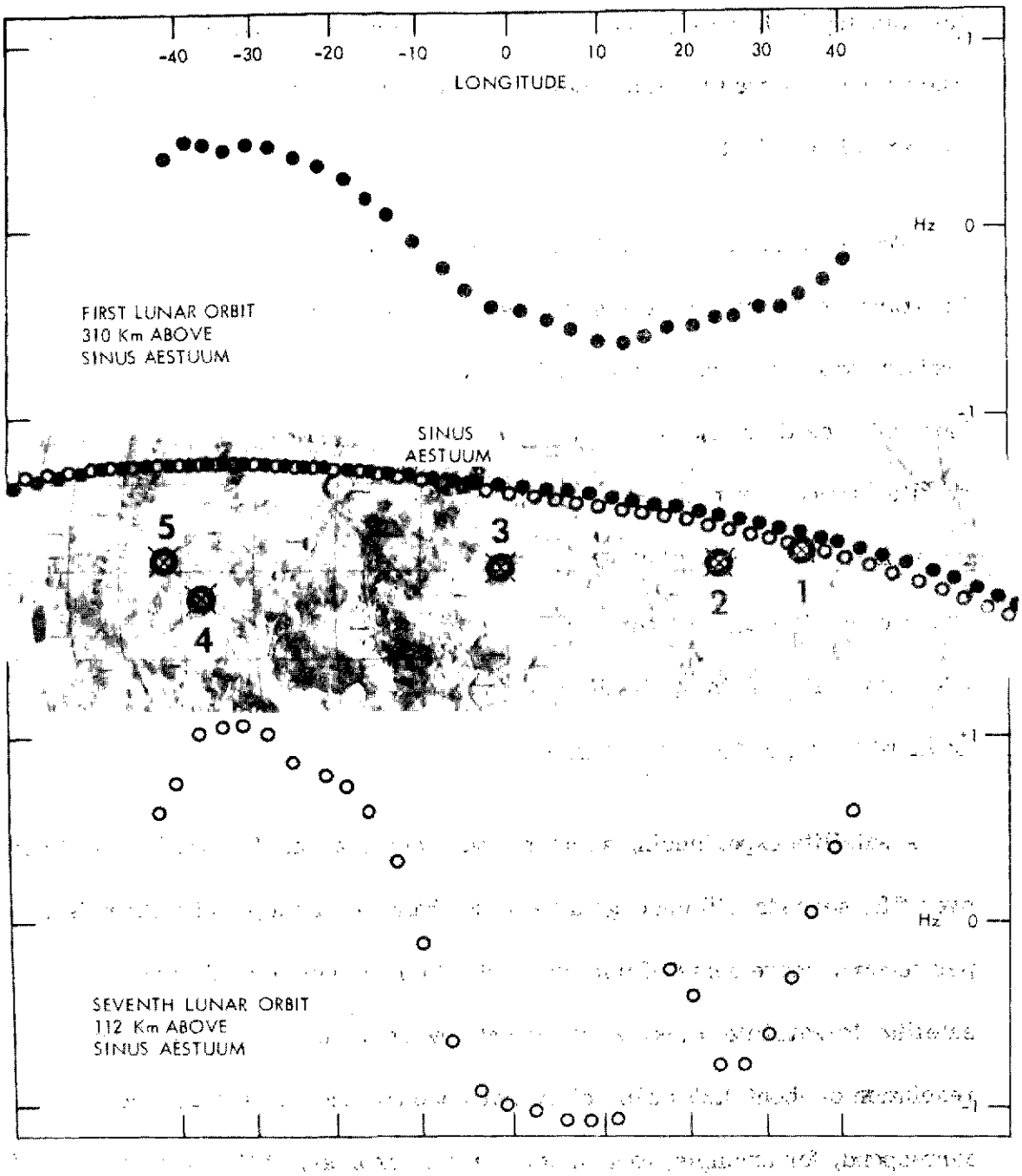

Figure 11. Doppler residuals from Lunar Orbits of Apollo VIII on December 24, 1968. The upper and lower portions of the figure depict residuals obtained in the neighborhood of Sinus Aestuum during the first and seventh revolutions, respectively. The residuals are plotted vs. position along the retrograde orbit. The positions in the two revolutions are indicated by surface tracks which are correspondingly marked in the central portion of the figure. The Apollo Lunar landing sites are also shown.

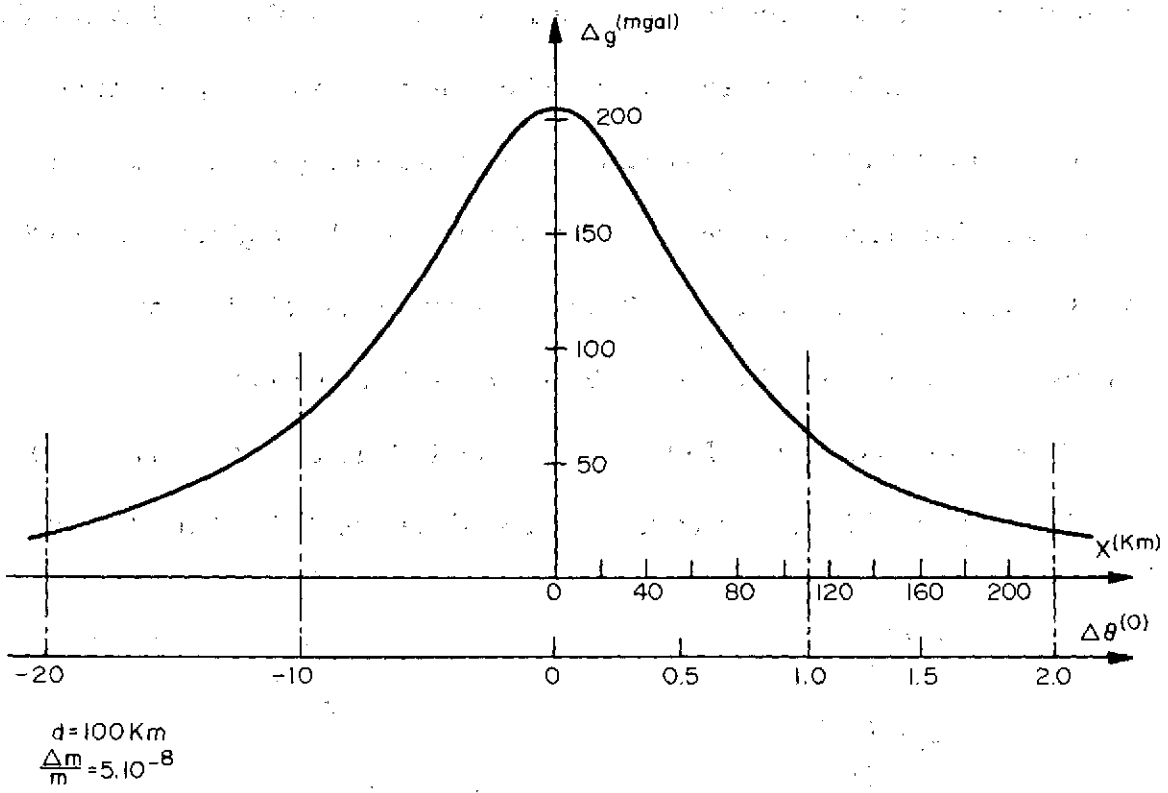

Figure 12

The tracking of a low altitude satellite such as GEOS-C from ATS-F is expected to yield information about the gravitational field which is more detailed in terms of space resolution than that obtainable from the existing sets of satellite data. The degree to which mean gravity anomalies in adjacent squares on the earth's surface can be separated on the basis of satellite-to-satellite tracking data of the ATS/GEOS-C type is a function of the altitude of the low satellite.

The dimensions of such a square are roughly comparable to the altitude of the low satellite. This problem has been studied in some detail by Schwartz (42).

Figure 13 depicts the relationship he found between the satellite altitude and the size of the square in which gravity anomalies can be identified by means of satellite-to-satellite tracking techniques. Extrapolation of this result to the general altitude region now planned for GEOS-C, i.e., the neighborhood of 900 to 1000 kilometers, leads to an estimate of approximately six degrees for the spatial resolution capability of the GEOS-C/ATS-F experiment.

The magnitudes of the effects are indicated in Figure 14 for a satellite in a 700 km altitude orbit. It is presently estimated that the ATS-F/GEOS-C tracking

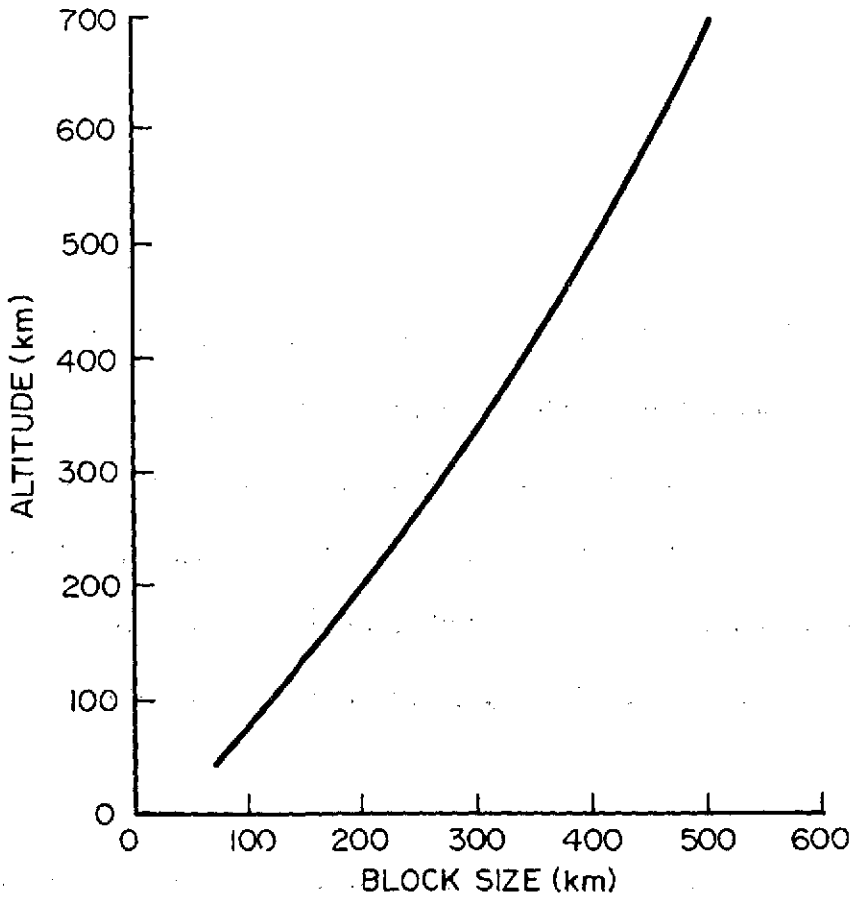

Figure 13

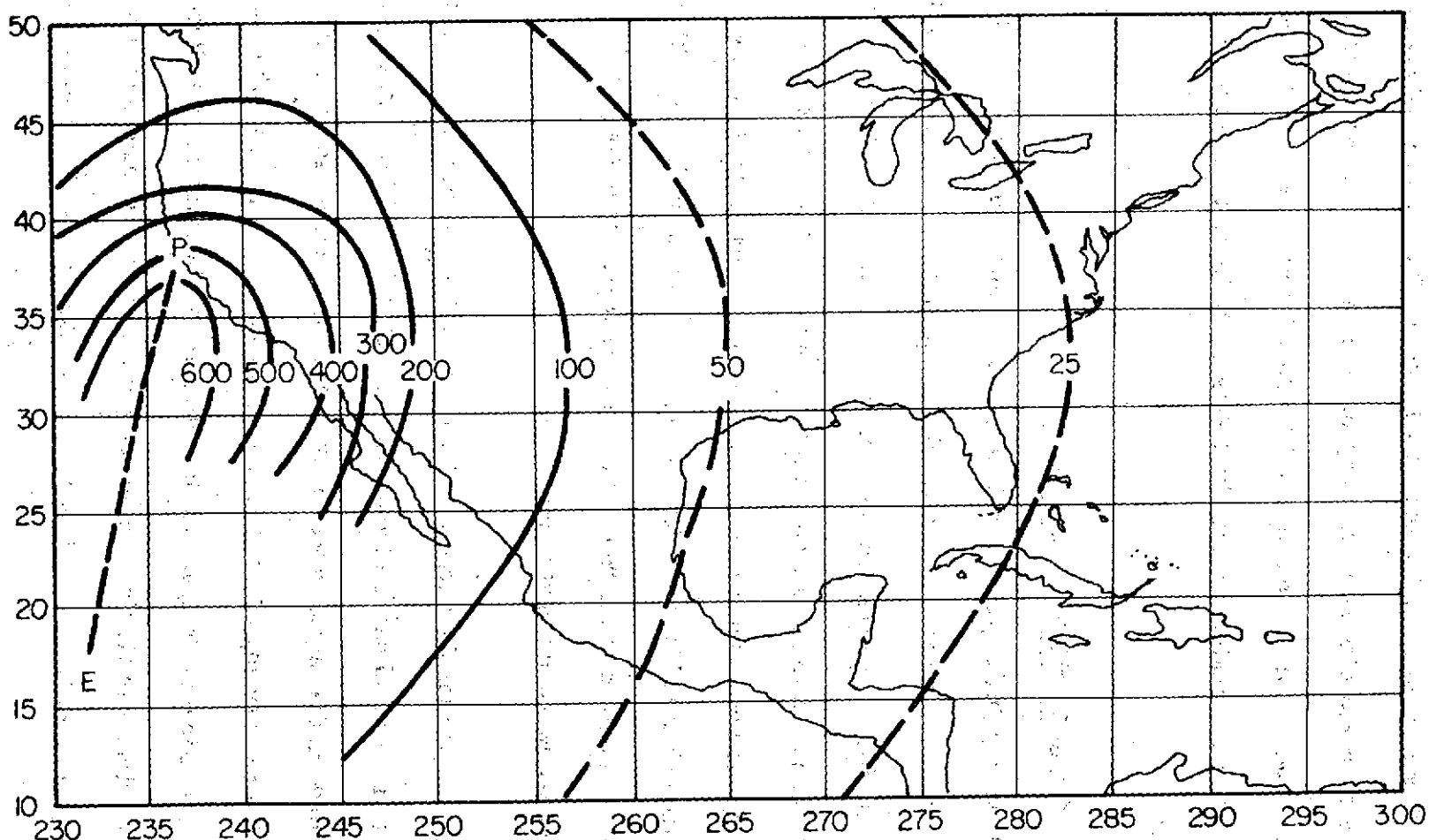
50
45
40
35
30
25
20
15
10
230
235
240
245
250
255
260
265
270
275
280
285
290
295
300
P
E
600
500
400
300
200
100
50
25

Figure 14

system will have an accuracy of about 0.35 mm/sec for a ten second integration time. The corresponding resolution capability in terms of a mean anomaly in a five-degree square for a satellite in a 700 kilometer altitude orbit is about 4.4 milligals. The implications of this for GEOS-C will be discussed further in Section IV.

2. GEOS-C Orbit Selection Considerations

It was originally planned that the GEOS-C orbit would have an inclination of about 20°. More recent thinking revolves around inclinations in the 40° to 65° range. A number of the conclusions derived on the basis of analyses conducted for the 20° case are valid also for higher inclinations. Some of these analyses, accordingly, will be described here. The following discussion is intended to indicate the different kinds of scientific objectives which can be met with a particular selection of a GEOS-C orbit. Most of these same thoughts also apply to inclinations in the 40° to 65° range.

It is assumed for the purpose of the case considered here that the GEOS-C orbit will have an inclination of approximately 115°, i.e., 65° retrograde, and a mean altitude in the neighborhood of 900 to 1000 kilometers, as was indicated above. The eccentricity will be taken to be 0.005 or less, a range which will simplify the altimeter design. One is at liberty to adjust the mean altitude or the period within certain limits in the attempt to achieve as many of the scientific goals as possible. The values finally selected will be governed partly by

considerations brought out in the following discussions. They may be somewhat different than those indicated here, however it is not anticipated that the principles underlying the present discussion will be fundamentally changed.

The spatial resolution obtainable with the satellite-to-satellite tracking data in an experiment of the GEOS-C/ATS-F type is about 5.7 degrees, as was indicated in the earlier discussion.

Starting from this point, one can work out the following orbit parameters which will accommodate the objectives of the Gravimetric Geodesy Investigation from the standpoints of the gathering of both the satellite-to-satellite tracking data and altimeter tracking data. It will be seen later that a number of important oceanographic objectives can also be met with the orbit selection which is discussed here.

An orbit having a 65° retrograde inclination, a mean altitude of approximately 1000 km and a corresponding period of about 105 minutes will move westward in longitude by about 26.2° each revolution. This orbit has ground track equator crossings which shift to the west about 6.3 degrees per day. The resulting separation between the orbit traces, which is smaller by the factor sin i, is 5.7° which corresponds to the value indicated above. The desired 5.7° survey pattern is thus approximately traversed in fifty-five revolutions of GEOS-C, in a bit more than four days. It includes a complete set of tracks, crossing the

equator in both the ascending and descending directions, separated by about 5.7 degrees.

At the beginning of the fifth day, the longitude of the ascending node of the 56th revolution is found to be displaced from that of the first revolution by about a degree, i.e., about a sixth of the daily shift. (Cf. Fig. 15) This can be thought of as the beginning of the phase in which the fine, or one-degree, pattern is laid down. The process continues for a total of 344 revolutions, at the end of which the ground track repeats, i.e., it is planned that the ground tracks of the first and the 345th revolutions will coincide. This, in fact, is the precise defining criterion for the orbit in the context of the chosen inclination, i.e., 65° retrograde, and eccentricity, namely, about 0.005. Thus, in something over 25 days, such a GEOS-C orbit will provide for an altimeter survey with orbits separated by slightly less than a degree. Since the altimeter cannot operate continuously, due to power limitations, an actual survey of this type would take much longer, on the order of a year, in fact. (43)

Clearly other strategies are possible, e.g., by selecting patterns which would give spacings of about 3°, 1.5°, etc. The example sketched here will suffice for the purposes of the present discussions, however. Resonances may be associated with some of these choices. A preliminary look at this point indicates that these will not be unduly severe, however. The degree to which such a specific fine resolution can be realized depends upon the launch vehicle capabilities.

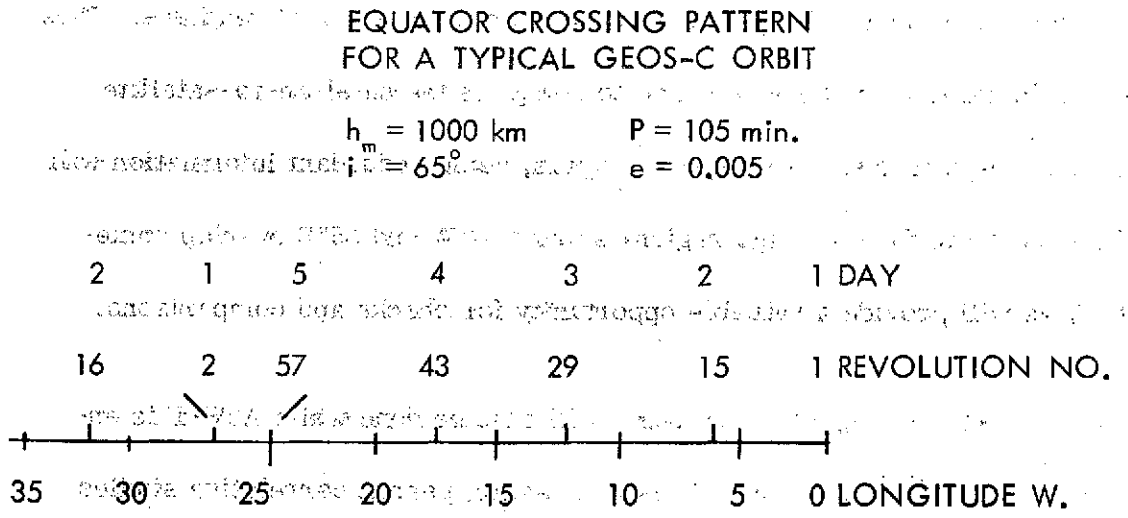

Figure 15

3. Satellite-to-Satellite Tracking Data Requirements

a. Gravimetric Geodesy Analyses

This information about the orbit furnishes the basis for estimating the data taking requirements. The 6.3 degree separation at the equator implies that some 57 passes will be trackable from ATS while it is in a fixed position.

Half of these correspond to ascending nodes, half to descending nodes. Each pass will be about 58 minutes long. Hence, a total of some 56 hours of satellite-to-satellite tracking will complete this six-degree survey. Redundant information will be obtained near the maximum latitudes since the tracks are less than 6 degrees apart. In an initial experiment, however, it is probably wise, even so, to plan on continuous satellite-to-satellite tracking which should aid considerably in the interpretation of the data.

ATS-F will be at 94° W longitude at first, and then at 35° E longitude. Thus some 112 hours in all will be required to complete the satellite-to-satellite tracking surveys in these two regions. Again, some redundant information will be obtained, since the coverage regions around 94°W and 35°E overlap somewhat. This will provide a valuable opportunity for checks and comparisons.

Some satellite-to-satellite tracking will also be done while ATS-F is enroute between these 2 locations. This will, again, permit correlative studies which will strengthen the overall results. Perhaps another 50 hours or so could be devoted to this phase of the activity.

b. Orbit Determination Studies

The satellite-to-satellite orbit determination experiment can involve data taking patterns such as those indicated in Figures 16 and 17.

These data sequences could presumably be abstracted from those indicated above for the scientific investigations. Accordingly, they would not necessarily involve the additional use of the GEOS-C/ATS-F satellite-to-satellite tracking resources.

B. Altimeter Data

1. Introduction

It was pointed out above that the altimeter will be useful for both gravimetric and oceanographic investigations and that, to a certain extent, these studies may be inter-twined.

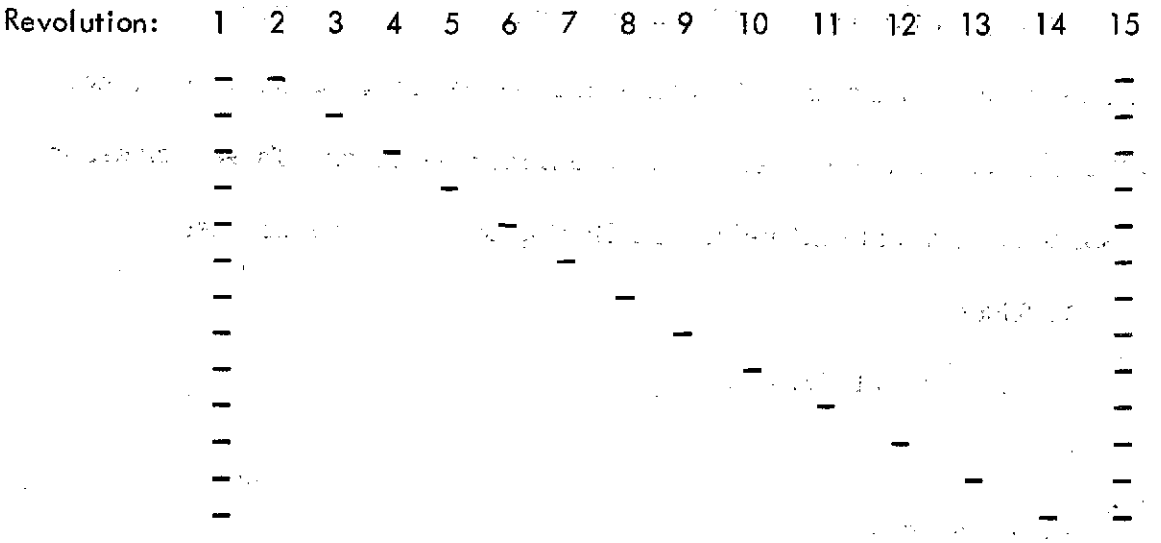

"—" ≡ One GEOS-C/ATS-F Satellite-to-Satellite Tracking Pass Spanning Half A Revolution.

Figure 16. Satellite-to-Satellite Tracking Data for Orbit Determination Analyses

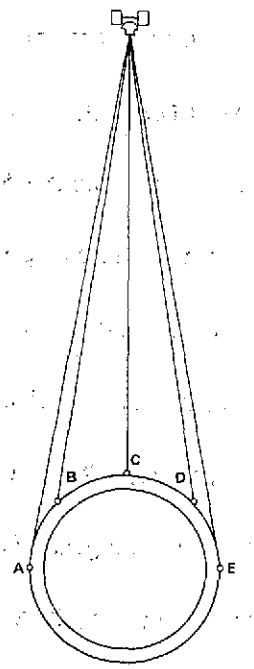

"o" ≡ A ONE-MINUTE GEOS-C/ATS-F SATELLITE-TO-SATELLITE TRACKING PASS. TRACKING PATTERNS SUCH AS THE FOLLOWING WOULD BE OF INTEREST: BD, BCD, ACE, & ABCDE.

Figure 17.

For example, the portion of the gravimetric geodesy investigation which is conducted with the aid of the altimeter will make use of the available knowledge of all of the factors which affect ocean height representation. These include, in addition to the gravitational field, the following oceanographic effects:

1. Tides
2. The General Circulation
3. Currents
4. Sea State
5. Storm Surges
6. Tsunamis

The following discussion is concerned partly with the representation of these oceanographic effects using available information. It is anticipated that each effect represented will also be investigated with the aid of the altimeter data. Thus the above list of oceanographic topics is both a list of effects to be represented, in connection with the gravimetric geodesy investigation, and a list of investigations to be conducted with the altimeter data. These various investigations are thus inter-related. In principle, with enough data, it should be possible to separate the gravitational effects, which are nearly invariant over the lifetime of the experiment, from the oceanographic ones, which vary with time in one way or another. In practice, however, it may be some time before enough data are available to make it feasible to effect such a separation without studying the data with both gravimetric and oceanographic thoughts in mind. In other

words, it may be advisable that the gravimetric and oceanographic analyses be viewed as coordinated or joint undertakings in some sense. The observational as well as the analytical aspects of the gravimetric and oceanographic investigations may also be approached jointly. The concept of a team of investigators considering both the gravimetric and oceanographic aspects of the problem may be appropriate here.

This discussion is aimed primarily at the gravimetric investigation and the representation of those oceanographic effects which are necessary in order to conduct the gravimetric investigation properly. Portions of the discussion that seemed to be especially likely to involve the possibility of joint planning such as those concerned with the observational programs, for example, do include suggestive thoughts relating to certain aspects of possible oceanographic investigations.

2. Ocean Surface Altitude and Satellite Position Representation

The representation of ocean surface altitudes and satellite positions will be considered in terms of the theoretical formulation, the organization of the calculations, and the specification of physical features associated with the gravitational and oceanographic aspects of the earth.

a. Theoretical Formulation

The theoretical formulation of the problem can be considered conveniently with the aid of the following definitions and relations:

$\underline{r}(t) \equiv$ spacecraft position vector

$\underline{h}_n(t) \equiv$ vector normal to reference ellipsoid extending from reference ellipsoid to spacecraft

$h_g \equiv$ height of geoid above ellipsoid of reference

$h_s \equiv$ height of sea surface above geoid

$\underline{R}_n(t) \equiv \underline{r}(t) - \underline{h}_n(t)$

$\underline{h}_g(t) \equiv h_g \ \underline{h}_n^*(t)$

$\underline{h}_s(t) \equiv h_s \ \underline{h}_n^*(t)$

$\underline{h}(t) \equiv \underline{h}_n(t) - \underline{h}_g(t) - \underline{h}_s(t)$

$h(t) \equiv |\underline{h}(t)|$

Functional dependences can be indicated further as follows, where the symbols have the meanings specified.

$$\underline{r}(t) = \underline{r}\{t, \ \underline{e}_0, \ GM, \ C_{nm}, \ S_{nm},$$

$$\rho(h, \ \varphi, \ \lambda, \ t, \ \odot_a, \ B_a),$$

$$\odot, \ \mathfrak{c}, \ \sigma, \ \pi, \ \gamma,$$

$$p.m., \ UT1, \ T_e\},$$

where

$$\underline{e}_0 \equiv (a, e, i, \Omega, \ \omega, m_0),$$

or

$$\underline{e}_0 \sim \underline{r}_0, \ \underline{\nu}_0,$$

GM GM = product of gravitational constant and mass of earth,

C_{nm}, S_{nm} = cosine and sine coefficients of spherical harmonic potential terms.

$\rho(h, \varphi, \lambda, t, \odot_a, B_a)$ = atmospheric density as a function of:

h: height

φ: latitude

λ: longitude

t: time

$\odot_a$: solar activity

B_a: magnetic activity

and where

$\odot$: solar gravitational field

$\mathbb{c}$: lunar gravitational field

σ: radiation pressure

π: precession

ν: nutation

p.m.: polar motion

UT1: earth's rotational position

T_e: earth tides

$$h_g = h_g \{C_{nm}, S_{nm}, g(\varphi_{ij}, \lambda_{ij}),$$

$$\mu_k, g(\varphi_{pq}, \lambda_{pq})\},$$

where the

$g(\varphi_{ij}, \lambda_{ij})$ denote gravitational anomalies specified in terms of latitude and longitude regions, the μ_k denote gravitational anomalies specified in terms of mascon parameters, and the $g(\varphi_{pq}, \lambda_{pq})$ denote gravitational anomalies specified

either directly or in terms of equivalent geoid heights at a number of latitude and longitude points.

Values at intermediate points are found by interpolation. The interval size will be specified as an integral multiple of a hundredth of a degree. The interval size may vary up to ten times over the range, and the interval patterns for latitude and longitude will be specified separately. Similar remarks apply to the specification of the order of interpolation. It is estimated that up to ten sets of the type $g(\varphi_{pq}, \lambda_{pq})$ containing a total of 10^5 functional values might be needed initially, and that each of these storage parameters might be an order of magnitude larger for more advanced studies.

The calculation of geoid height quantities, which are based on gravitational field expressions, could be implemented in more than one way. It could be done, for example, by evaluating these expressions at each point of interest. It could, alternatively, be done by evaluating these expressions at a specified set of times, e.g., at the times corresponding to those employed in the numerical integration processes, and by employing numerical procedures to calculate the geoid height quantities at the points of interest. The method could be optimized keeping in mind numerical analysis and computational efficiency considerations.

One or more specified sets of the quantities $g_m(\varphi_{pq}, \lambda_{pq})$, e.g. those associated with features such as trenches, say, would be multiplied by factors, k_m, respectively, which would initially have the value unity, but would be solved for as un-

known parameters. Ten to a hundred such quantities could be of interest. Thus, e.g.,

$$h_g = h_g \left\{C_{nm},\ S_{nm},\ g(\varphi_{ij},\ \lambda_{ij}),\ \mu_k\right\} + \sum_{m=1}^{n} k_m\, g_m\,(\varphi_{pq},\ \lambda_{pq}).$$

$$h_s = h_s \left\{T_e,\ T_0,\ h_0\ (\varphi_{pq},\ \lambda_{pq})\right\},$$

where T_0 denotes ocean tides and the $h_0(\varphi_{pq},\ \lambda_{pq})$ denote heights above the geoid of oceanographic and meteorological features, such as currents, tsunamis, and wind and pressure fields, specified at a number of latitude and longitude points. The remarks about interpolation, intervals, arrays and unknowns, k_m, made in connection with the functions $g(\varphi_{pq},\ \lambda_{pq})$, etc., apply in analogous fashion to the functions $h_0(\varphi_{pq},\ \lambda_{pq})$, etc. Other functions may also be used to represent oceanographic and meteorological phenomena. $\underline{R}_n(t) = \underline{R}_n(t,\ R_e,\ f)$, where R_e denotes the mean equatorial radius, and f denotes the flattening.

The quantities $\underline{r}$, h_g, h_s, and $\underline{R}_n$, will in general, be functions of unknown parameters which can be identified or associated with the indicated arguments. These unknowns, and any others involved, will be denoted here simply by x_i. The partial differential coefficients can be found with the aid of methods and expressions employed in systems such as the GTDS, the Goddard General Orbit Determination System, Geostar, etc. That which is obtainable involves the use of numerical differentiation, numerical integration, or analytic theory, as appropriate.

$$\frac{\partial h}{\partial x_i} = \frac{\partial \underline{r}}{\partial x_i} \cdot \underline{h}^* - \frac{\partial \underline{R}_n}{\partial x_i} \cdot \underline{h}^* - \frac{\partial h_g}{\partial x_i} - \frac{\partial h_s}{\partial x_i}.$$

Here, for example,

$$\frac{\partial h_g}{\partial k_m} = g_m(\varphi_{pq}, \lambda_{pq}),$$

for m = 1, 2, . . . , n.

$\partial h/\partial x_i$ can be derived, for example, numerically by differencing over a suitable time interval, e.g., one which corresponds to the measurement interval. The determination of the time to be associated with the derived quantity can be made by an appropriate method. Alternatively, such a measure may be regarded directly as a height difference over a finite time interval and treated accordingly.

b. The Organization of the Calculations

The organization of the partial derivative calculations is indicated in Figure 18 and Table IX. The notation of Figure 18 corresponds to that employed in reference 33.

C. The Specification of Physical Features

Analysis of the altimeter data involves the representation of the gravitational field and of the types of oceanographic effects which were listed above in the introduction to this section.

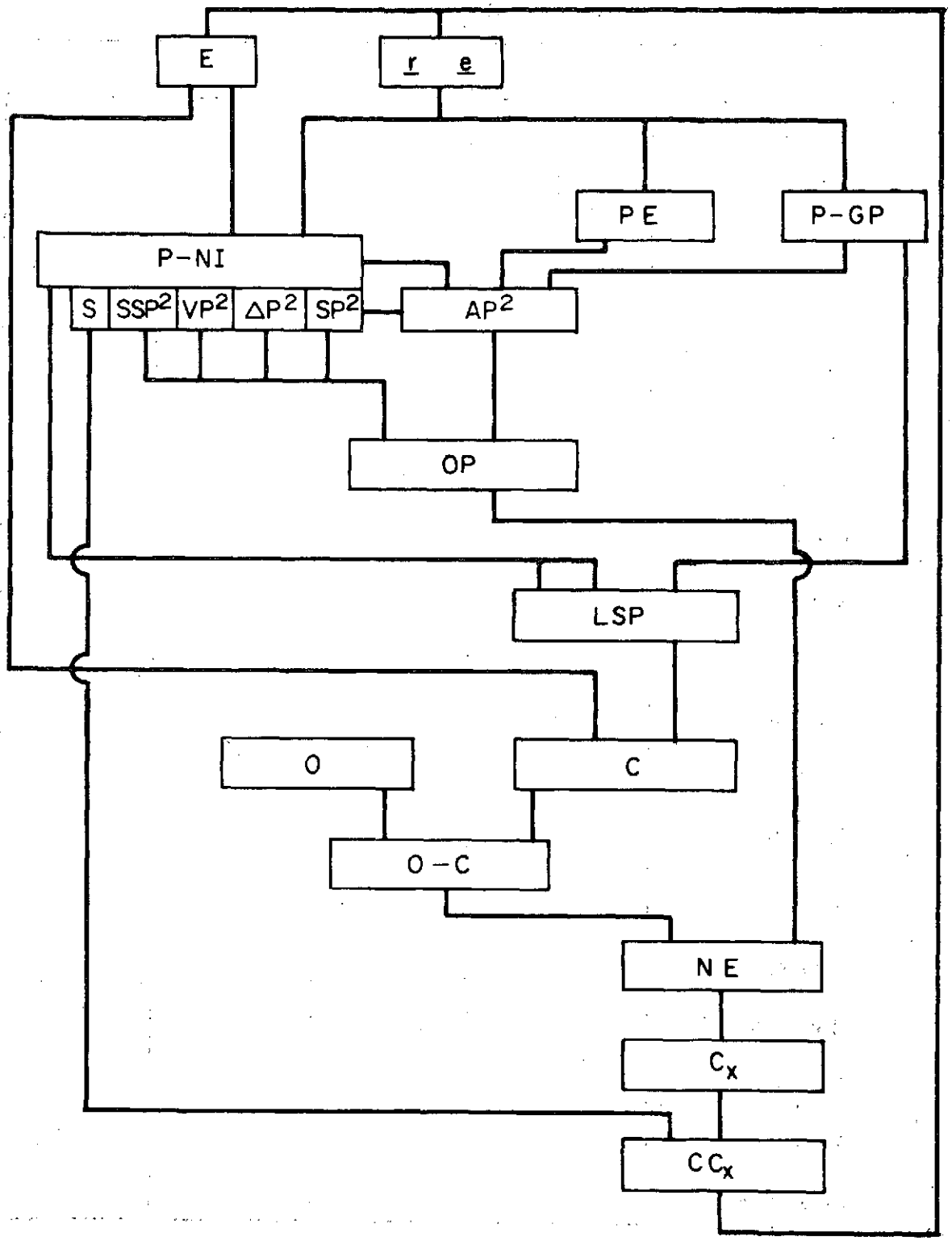

Figure 18

Table IX

	$\underline{r}$	$\underline{R}_n$	h_g	h_s
$a\ e\ i\ \Omega\ \omega\ M_0$	✓			
GM	✓			
$C_{nm}\ S_{nm}$	✓		✓	
$\rho\ \sigma$	✓			
$\odot\ \mathbb{C}$	✓			
$\pi\ \nu$	✓			
PM UT1	✓			
Tides	✓			✓
Anomalies	✓			
Regions	✓		✓	
Mascons	✓		✓	
Features	✓		✓	
Trenches	✓		✓	
Ref.		✓		
Currents				✓
Storm Surges				✓
Tsunamis				✓
Winds				✓
Pressures				✓

It will be assumed for the purposes of this portion of the discussion that the GEOS-C altimeter will be capable of instrumental resolution at the 2 meter level in one mode and at the 0.5 meter level in a second mode.

i. The Geoid

The broad features of the geoid are given by satellite analysis. The best representation currently available is the one presented by SAO seen in Figure 19.

Detailed studies of the geoid in certain regions have been conducted by a number of investigators including Von Arx, Talwani, Uotila, Rapp, Strange, Vincent, Berry, and Marsh. (44-48.) An indication of the availability of results in several regions of interest off the East and Gulf Coasts of the United States is

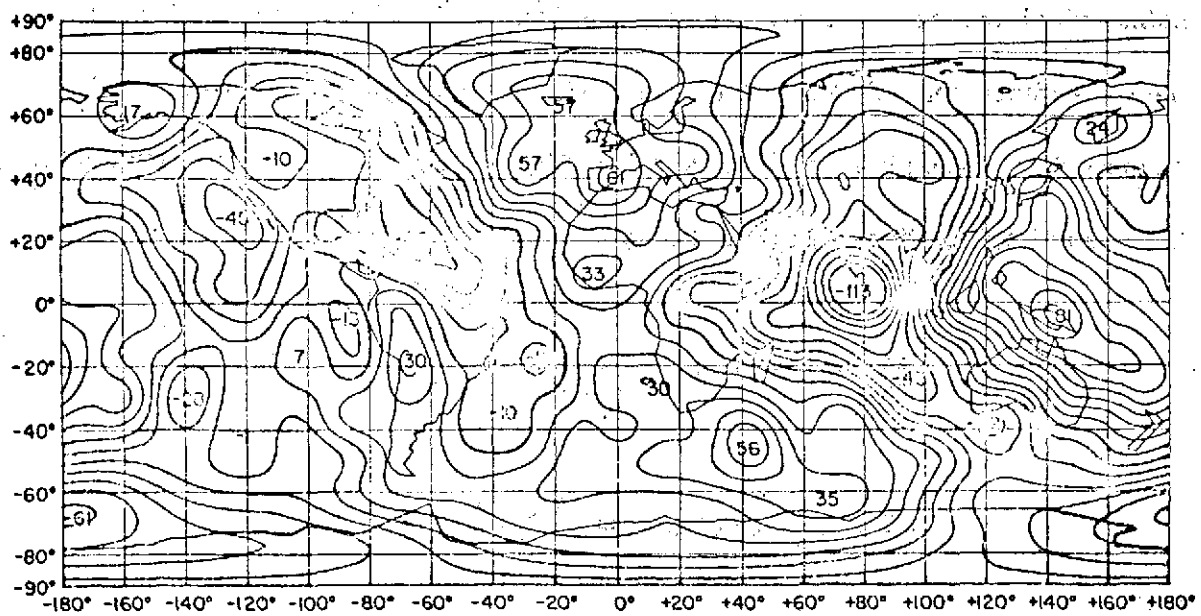

Figure 19. Geoid heights in meters of the new combination solution corresponding to a reference ellipsoid of flattening f = 1/298.255.

presented in Figure 20. An example of such a detailed geoid, and a satellite geoid for the same region, are seen in Figures 21 and 22. (49, 18.) It is understood that further detailed geoidal results will be forthcoming in the relatively near future (50).

ii. Tides

The departure of the ocean surface from the geoid can be thought of in terms of tidal phenomena and the features of the general circulation, including current patterns and more variable features associated with currents such as the meanders of the Gulf Stream.

Tidal phenomena have been studied by Hendershott, Munk and Zetler (51, 52). Hendershott and Munk describe a model involving a number of amphidromic points which can be obtained by solving the Laplace Tidal Equations (LTE) in the case where coastal values are given. (Cf. Figure 23). Cotidal lines for the Atlantic Ocean are given in more detail in Figure 24 which is due to Hansen (53). The basic Laplace tidal equations are given by:

$$\frac{\partial u}{\partial t} - (2\Omega \sin\theta)\, v = \frac{-g}{a\cos\theta}\,\frac{\partial(\zeta - \overline{\zeta})}{\partial\phi},$$

$$\frac{\partial v}{\partial t} + (2\Omega \sin\theta)\, u = \frac{-g}{a}\,\frac{\partial(\zeta - \overline{\zeta})}{\partial\theta},$$

and

$$\frac{\partial\zeta}{\partial t} + \frac{1}{a\cos\theta}\left(\frac{\partial(uD)}{\partial\phi} + \frac{\partial(vD\cos\theta)}{\partial\theta}\right) = 0$$

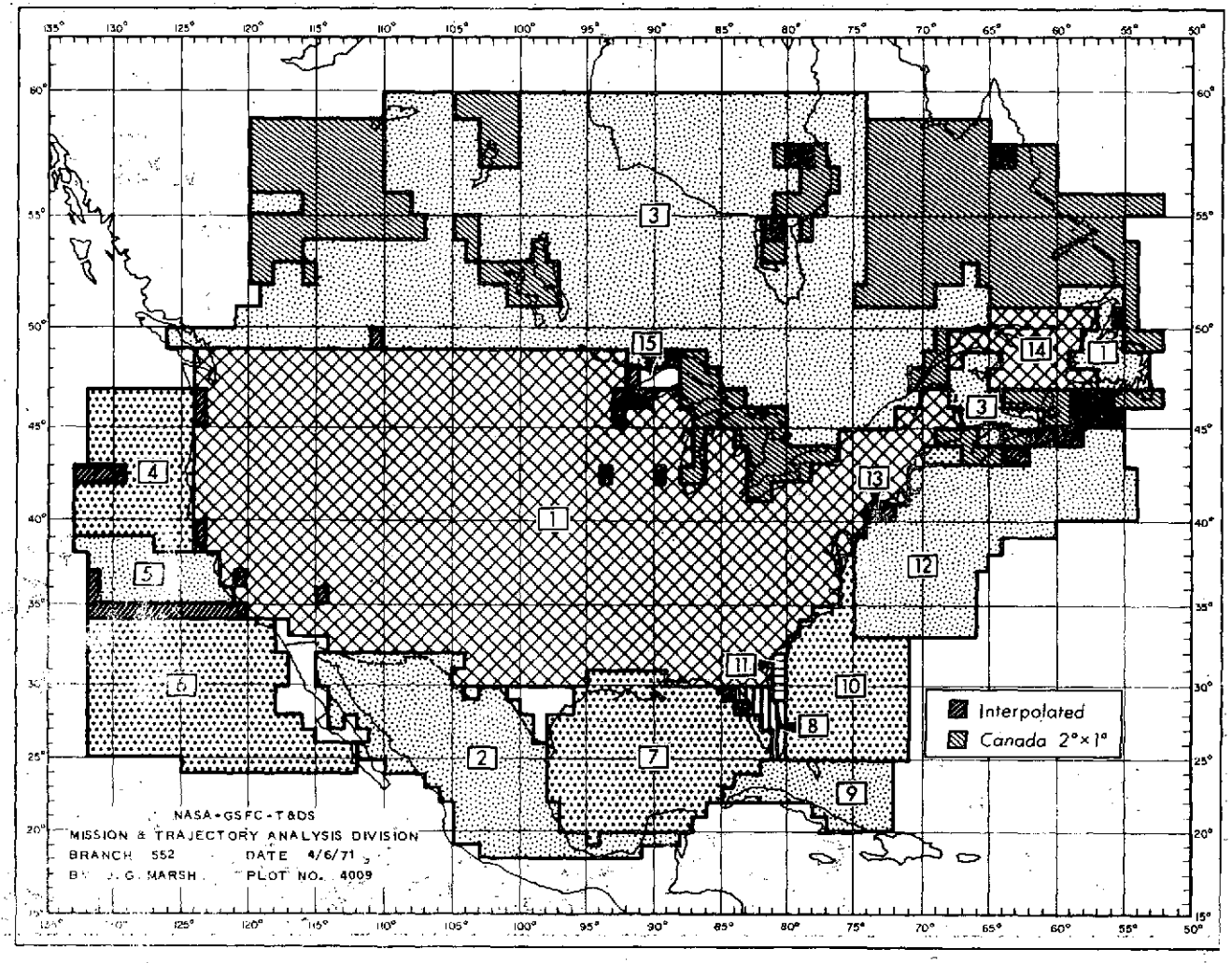

Figure 20. Area of Surface Gravity Coverage

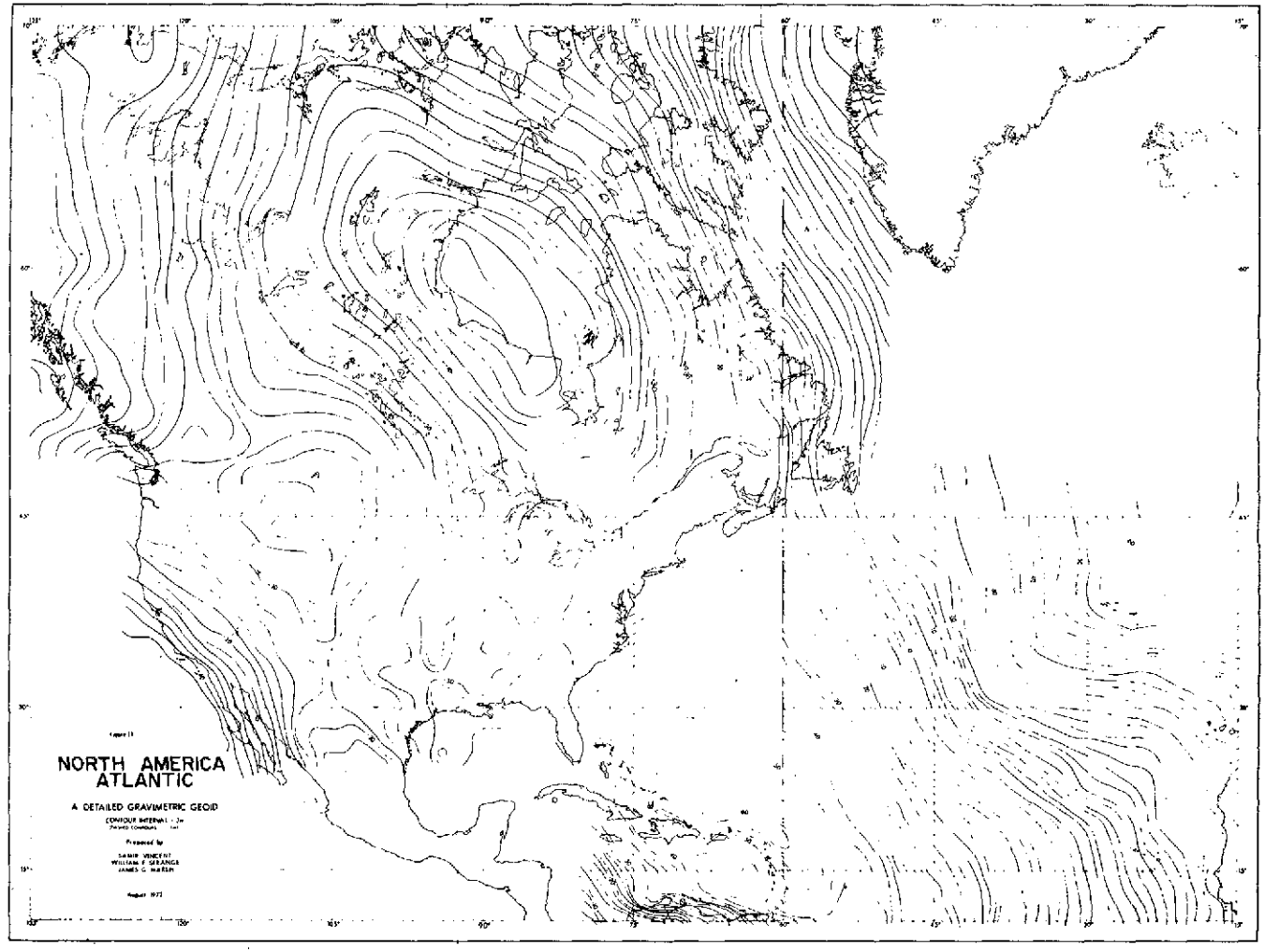

Figure 21. Detailed Gravimetric Geoid

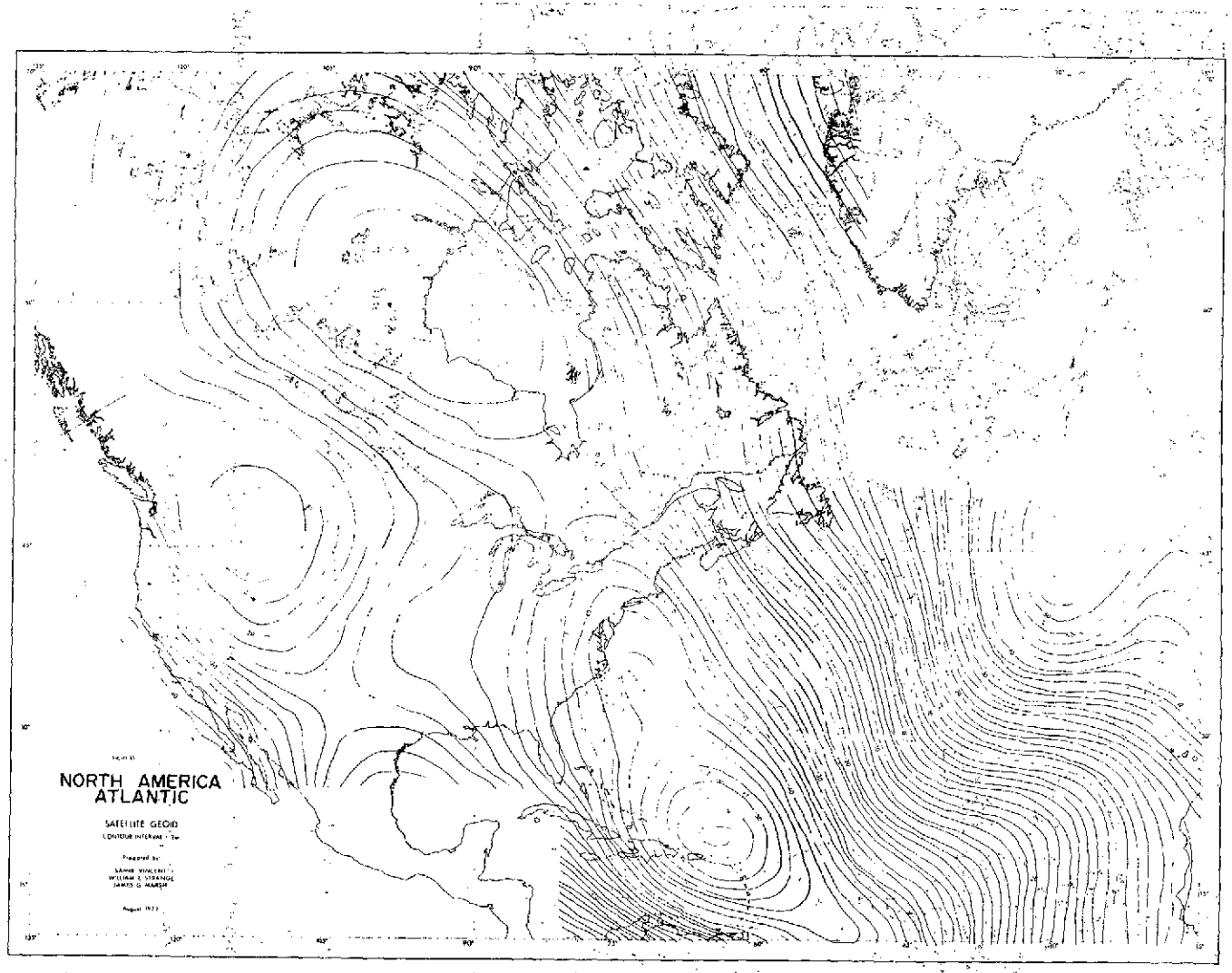

Figure 22

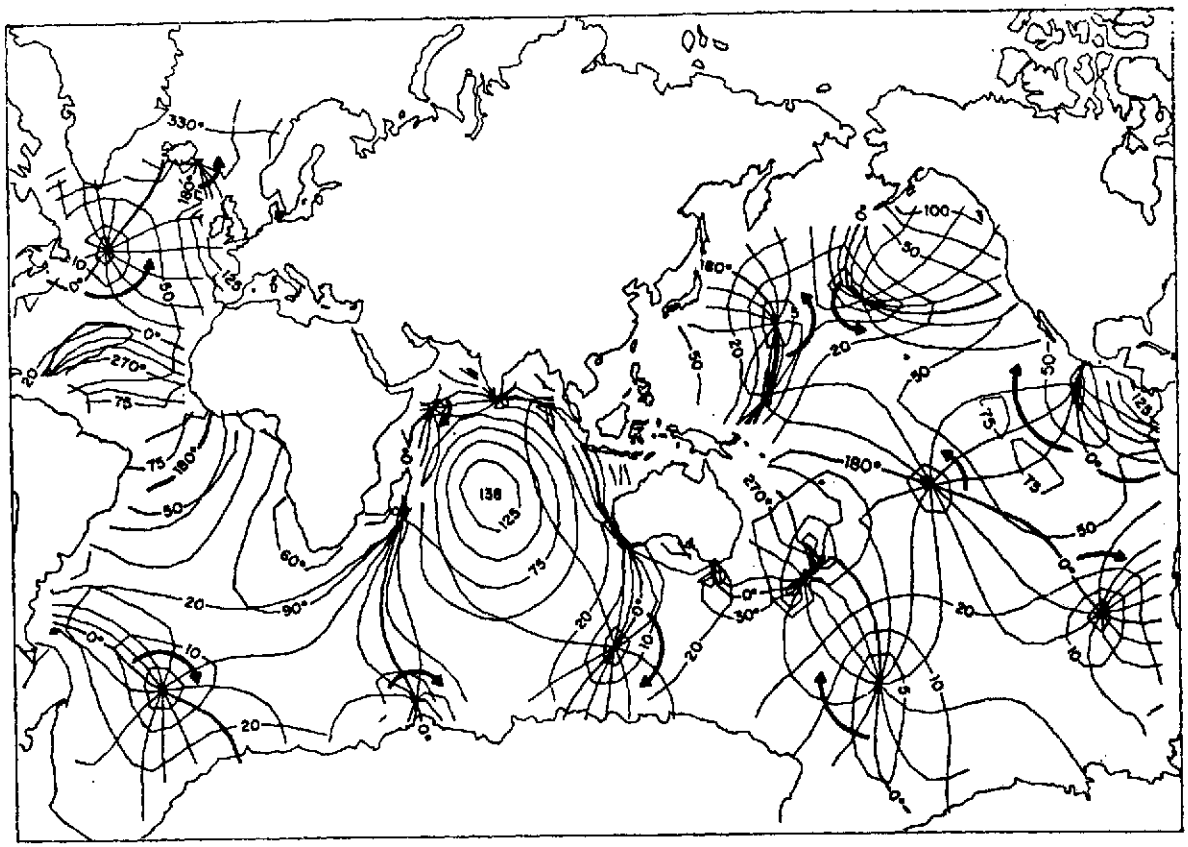

Figure 23

They have been studied in a number of simplified forms.

Hendershott's recent research has extended them to include effects of solid earth tides which he found to be significant (54).

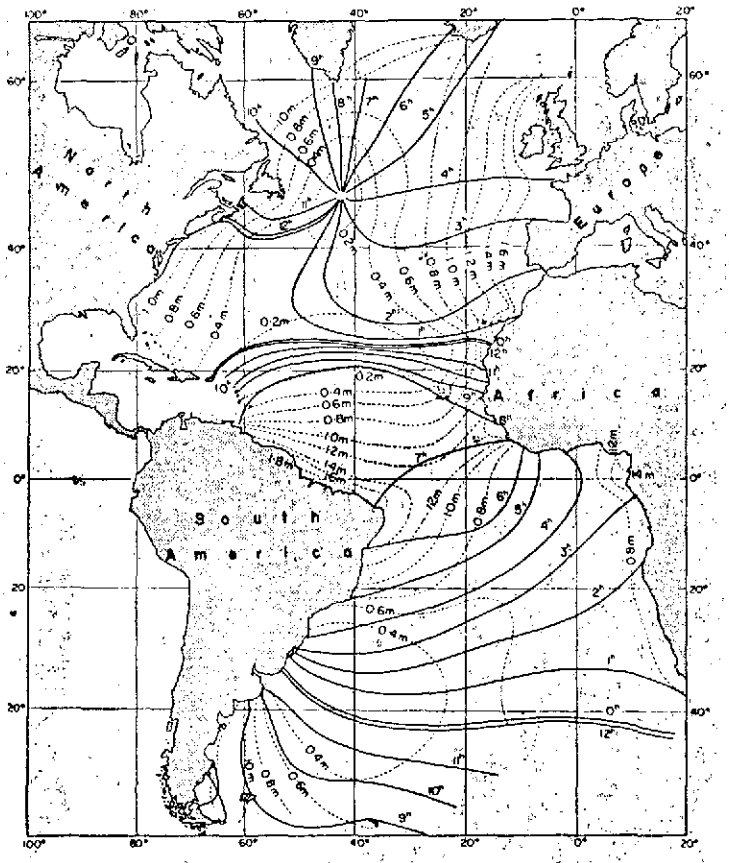

Figure 24. Theoretical tides of Atlantic Ocean. Full lines: co-tidal lines referred to moon-transition through meridian of Grw., dashed lines: co-range lines of the semi-diurnal tide M_2 in m (according to Hansen).

iii. The General Circulation of the Oceans

Problems associated with the general circulation have been discussed by H. Stommel, K. Bryan and Hansen. (Cf. references 55 and 56.)

A model for the world-wide general circulation has been presented by Stommel. It appears in Figure 25. More detailed studies of particular regions such as the North Atlantic are being conducted by Bryan and Hansen (56).

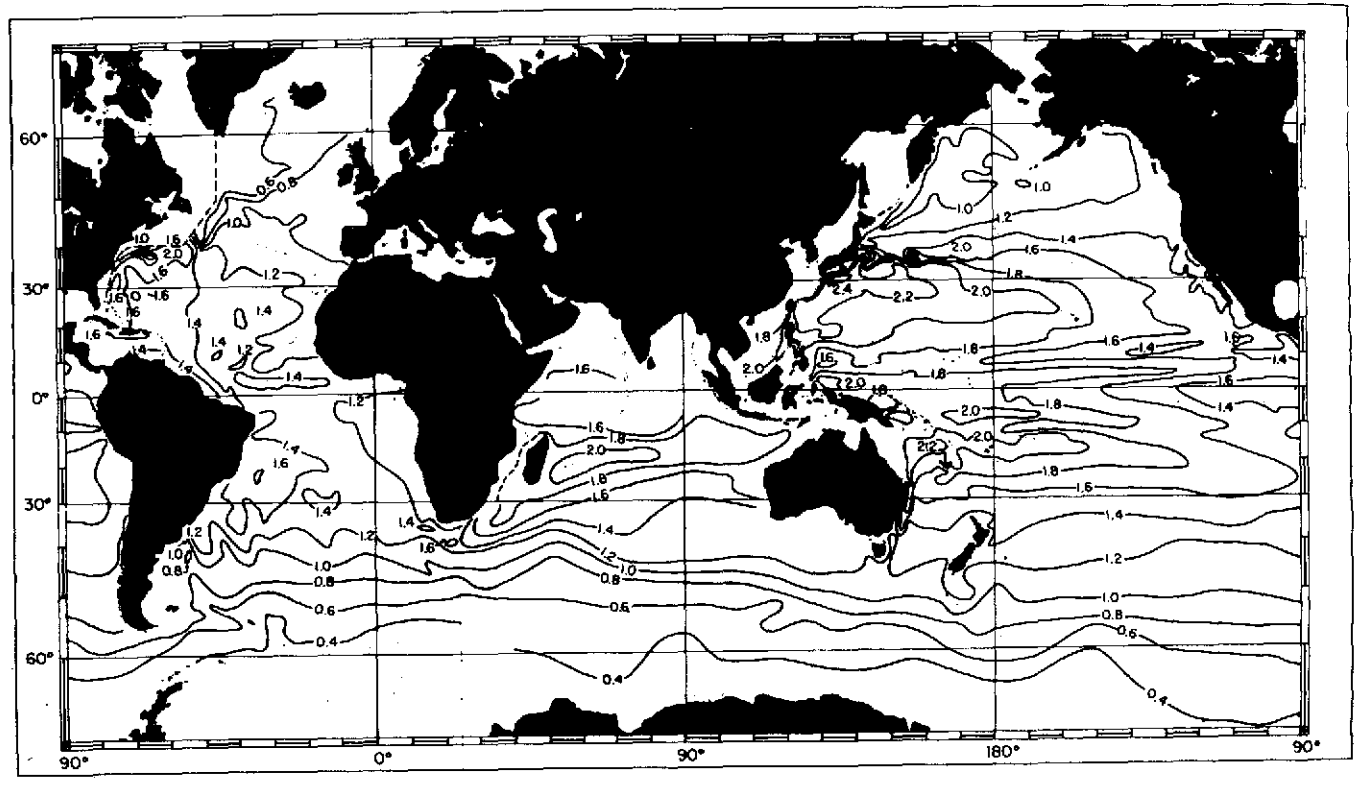

Figure 25. Dynamic Topography of the Sea Surface relative to the 1000-Decibar Surface.

iv. Currents

The general circulation embraces a number of major current systems including the Gulf Stream, the Kuroshio Current near Japan, and the Antarctic circumpolar current.

The Gulf Stream is of special interest here for several reasons including the fact that it meanders.

- The Gulf Stream Meanders

Considerable effort has been devoted to the study of the meanders of the Gulf Stream. This research is discussed by Hansen (57). The Gulf Stream proper can be thought of as a Kelvin wave. Departures from this model are also of interest here.

In the study described by Hansen, the position of the Gulf Stream between Cape Hatteras and approximately 60° west longitude was observed at intervals ranging from a few days to a month. The 15° isotherm was chosen as an index of the main thermal front at a depth of 200 meters, and hence as an indication of the Gulf Stream position (57).

Wavelike features having wavelengths of 200-400 km were observed. Hansen shows them in Figure 26. The evolution of the meanders in terms of phase progression is indicated in Figure 27. It is seen there that the meanders progress at a rate of the order of a mean wavelength, taken to be 300 km, each couple of months. This corresponds to about 5 km/day.

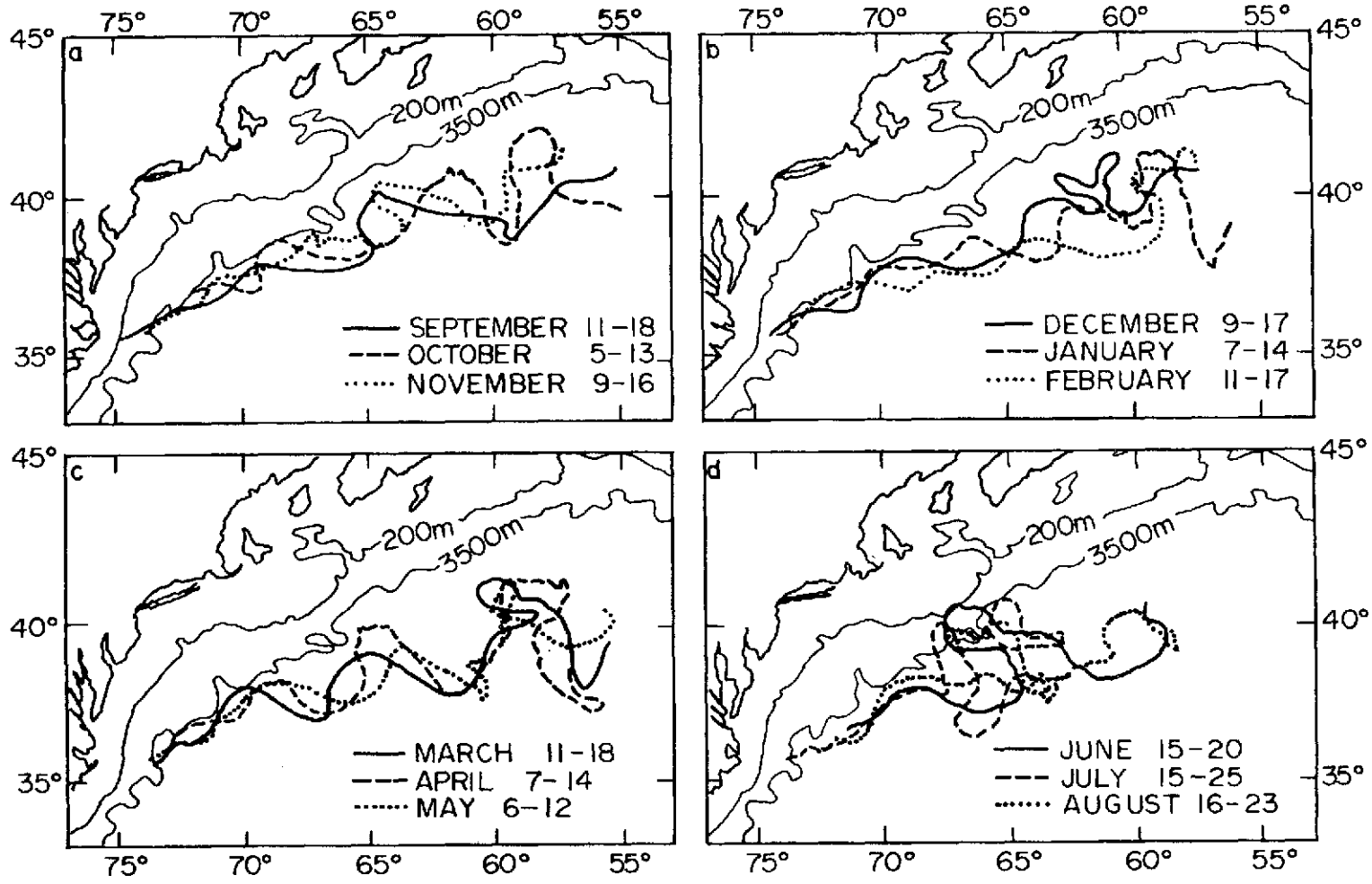
a
b
c
d
75°
70°
65°
60°
55°
45°
40°
35°
200m
3500m
SEPTEMBER 11-18
OCTOBER 5-13
NOVEMBER 9-16
DECEMBER 9-17
JANUARY 7-14
FEBRUARY 11-17
MARCH 11-18
APRIL 7-14
MAY 6-12
JUNE 15-20
JULY 15-25
AUGUST 16-23

Figure 26

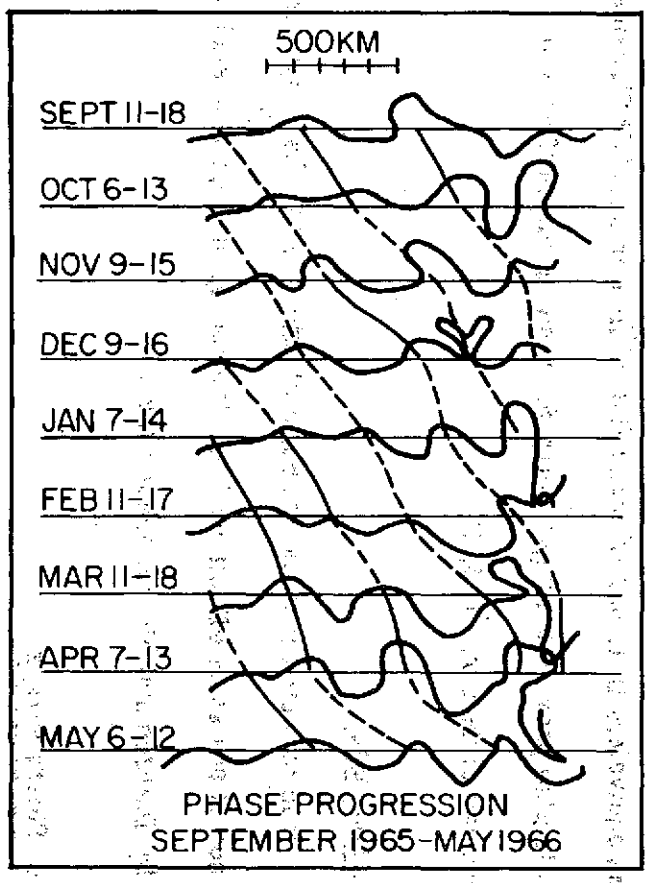
500KM
SEPT 11-18
OCT 6-13
NOV 9-15
DEC 9-16
JAN 7-14
FEB 11-17
MAR 11-18
APR 7-13
MAY 6-12
PHASE PROGRESSION
SEPTEMBER 1965-MAY 1966

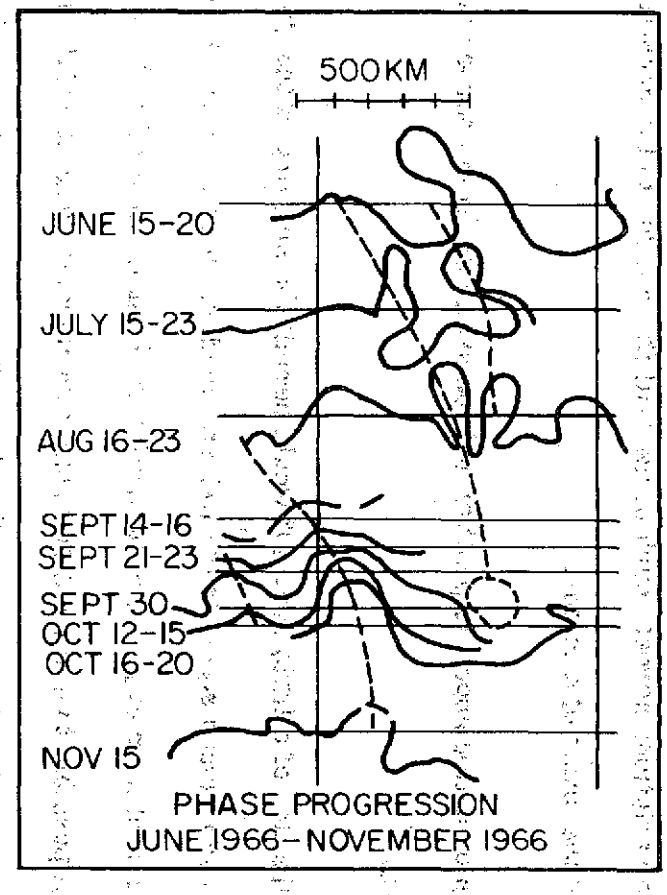
500KM
JUNE 15-20
JULY 15-23
AUG 16-23
SEPT 14-16
SEPT 21-23
SEPT 30
OCT 12-15
OCT 16-20
NOV 15
PHASE PROGRESSION
JUNE 1966-NOVEMBER 1966

Figure 27.

Altitude variations across much of the Gulf Stream due to the geostrophic effect are of the order of a meter.

Some information about its position will be available from sources other than GEOS-C.

An inclination of a little over 40° would permit the studying of the Gulf Stream meanders and also of other western boundary currents such as the Kuroshio current near Japan. An inclination in the neighborhood of 65° would also make it possible to study the antarctic circumpolar current which is of interest for more than one reason. It is the only continuous current which corresponds to a closed circuit or curve on the globe. It is also the strongest current being equivalent in terms of mass flux to five or six Gulf Streams. The 65° orbit would also provide good geometry for viewing the Gulf Stream. This point is discussed in Section III, 4, C.

v. Sea State

It is expected that the problem of interpreting the range measures in the presence of sea state effects will be attacked by an approach such as the one offered by Pierson and his colleagues (58).

vi. Storm Surges

Storm surges, such as those associated with hurricanes, for example, can have amplitudes of up to a couple of meters and wavelengths of some fifty kilometers.

Phenomena such as storm surges will be represented and/or observed when and where they occur, to the extent that this is practicable.

vii. Tsunamis

Tsunamis are thought to have amplitudes of nearly half a meter and wavelengths of perhaps three hundred kilometers. Detailed theoretical representation of a tsunami involves the representation of the ocean bottom topography and complex ray-tracing calculations to map out the advance of the expanding wave. The occurrence of a tsunami in a region and at a time when it might be observed by GEOS-C would be a relatively rare event. It could, however, be modeled and studied in this way.

3. The Calibration of the Altimeter

a. Short-Arc Tracking of GEOS-C in the Caribbean Area

The consideration of short-arc and long-arc tracking error budgets can begin with a look at the overall error problem. A typical error breakdown for the GEOS-C altimeter is indicated in Table X (59). Quantities associated with factors other than the orbit errors have an rms value of approximately 3 meters. This leaves 4 meters or so which can be assigned to the calibration process if the 5 meter rms overall accuracy goal is to be met. Allowing 1 or 2 meters for uncertainties associated with the geoid means that the uncertainties associated with the orbit determination process should contribute no more than about 3.5 meters.

Table X

GEOS-C Mission Altimeter Evaluation

Satellite Altimeter System Measurement Error Source	Error (m)
Altimeter Instrumentation	2
Refraction	0.2
Reflection from Waves	0.5
Spacecraft Attitude	2
Root Sum square	2.9
Calibration Error Allocation	4.1
Altimeter System	5
Evaluation Goal	

If comparable accuracies are to be achieved over extensive areas, the accuracy within a short-arc calibration region such as the one in the Caribbean must be increased still further. This point will be discussed further below.

A detailed analysis of short-arc tracking using lasers and cameras in the Caribbean area has been conducted by Berbert and Loveless (60). A GEOS-C ground track for the 22° inclination case in the neighborhood of several possible tracking locations in the Caribbean is seen in Figure 28. Elevation angles as functions of time for four of these sites for an orbit at a mean height of about eight hundred nautical miles are seen in Figure 29. The durations of the corresponding tracks above an angle of about 48° are indicated in Figure 30.

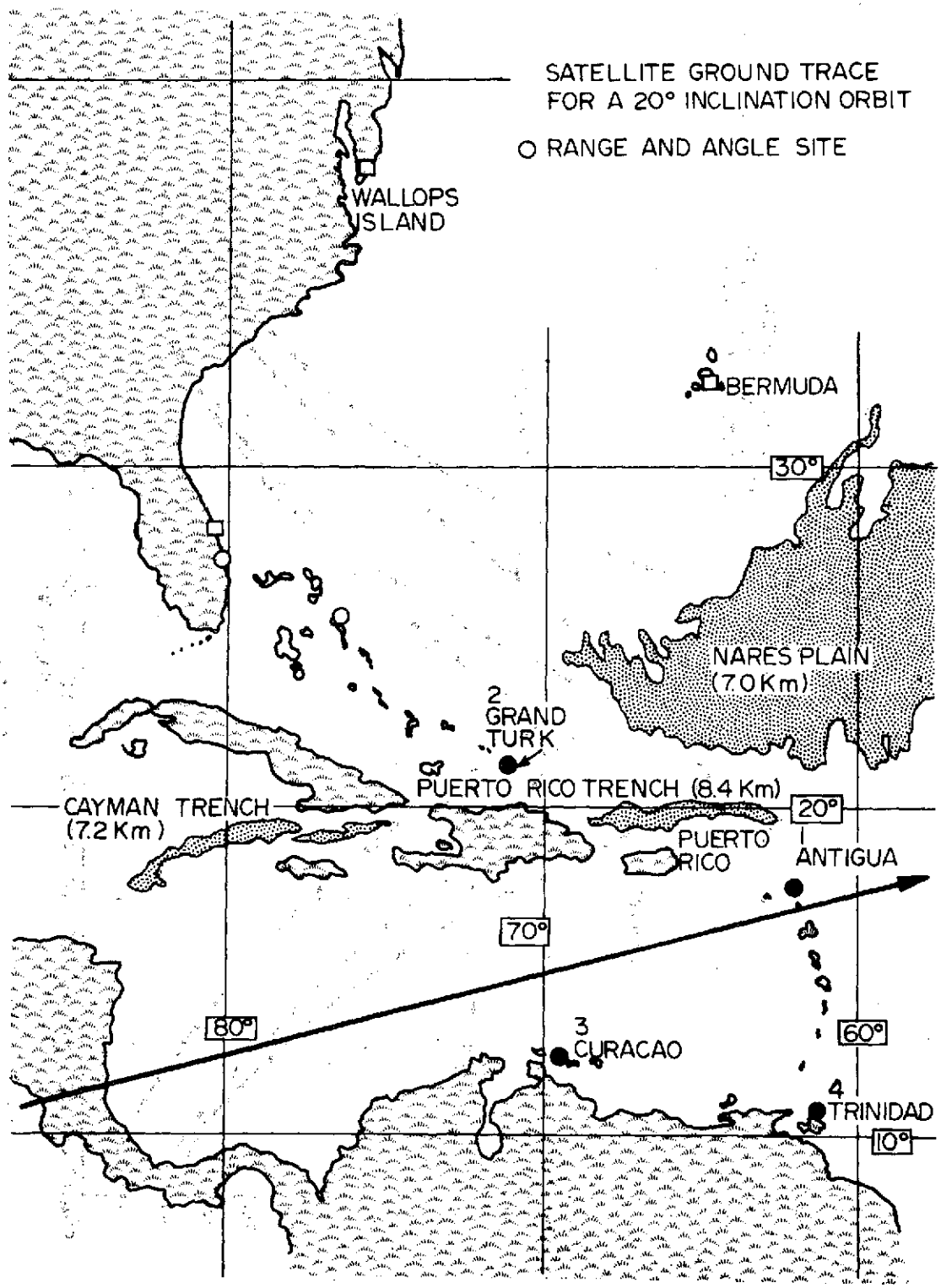
SATELLITE GROUND TRACE
FOR A 20° INCLINATION ORBIT
O RANGE AND ANGLE SITE
WALLOPS
ISLAND
BERMUDA
30°
NARES PLAIN
(7.0 Km)
2
GRAND
TURK
PUERTO RICO TRENCH (8.4 Km)
CAYMAN TRENCH
(7.2 Km)
20°
PUERTO
RICO
ANTIGUA
70°
80°
3
CURACAO
60°
4
TRINIDAD
10°

Figure 28

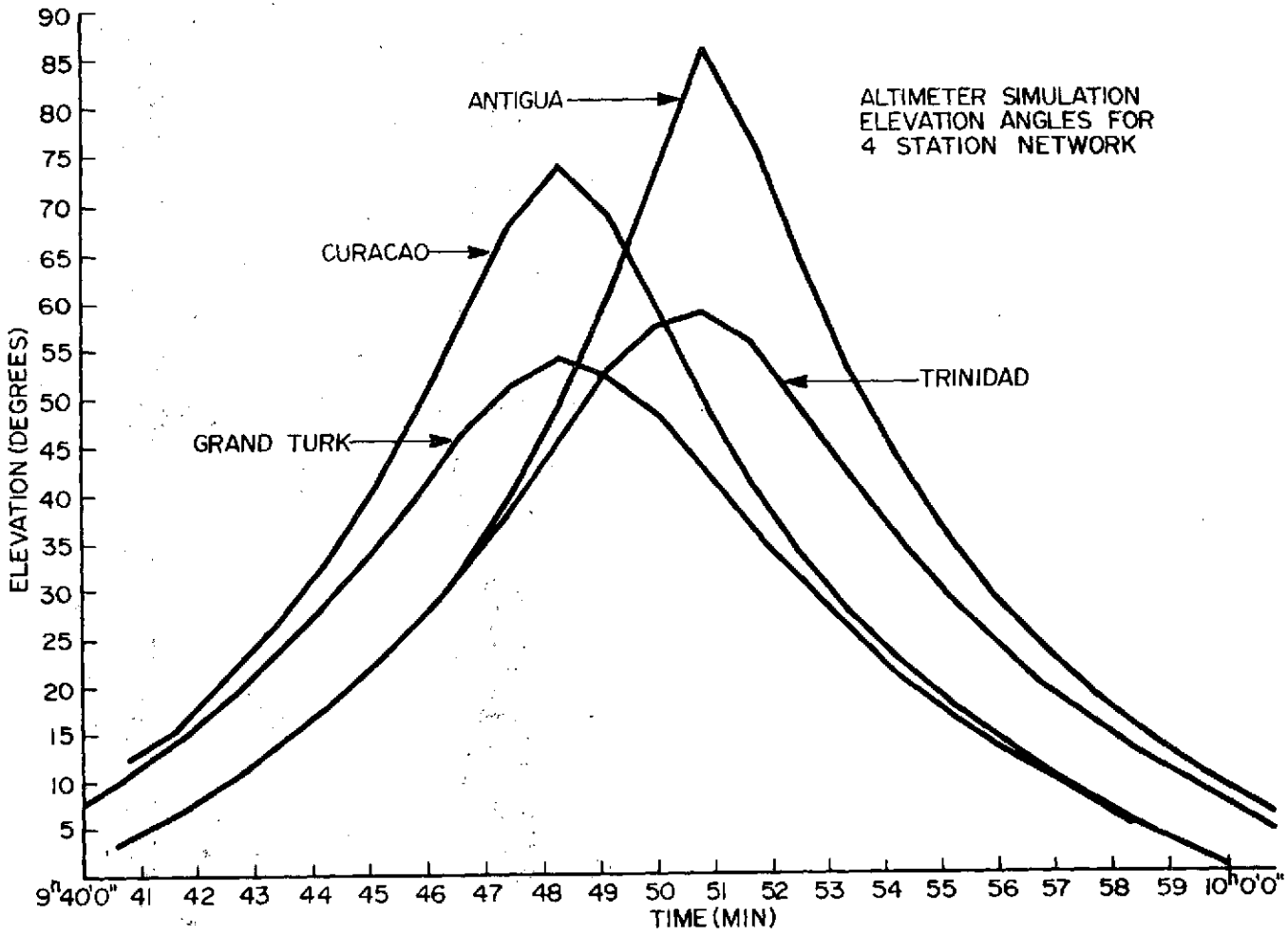
ALTIMETER SIMULATION
ELEVATION ANGLES FOR
4 STATION NETWORK
ANTIGUA
CURACAO
GRAND TURK
TRINIDAD
ELEVATION (DEGREES)
90
85
80
75
70
65
60
55
50
45
40
35
30
25
20
15
10
5
9h40'0" 41 42 43 44 45 46 47 48 49 50 51 52 53 54 55 56 57 58 59 10h0'0"
TIME (MIN)

Figure 29

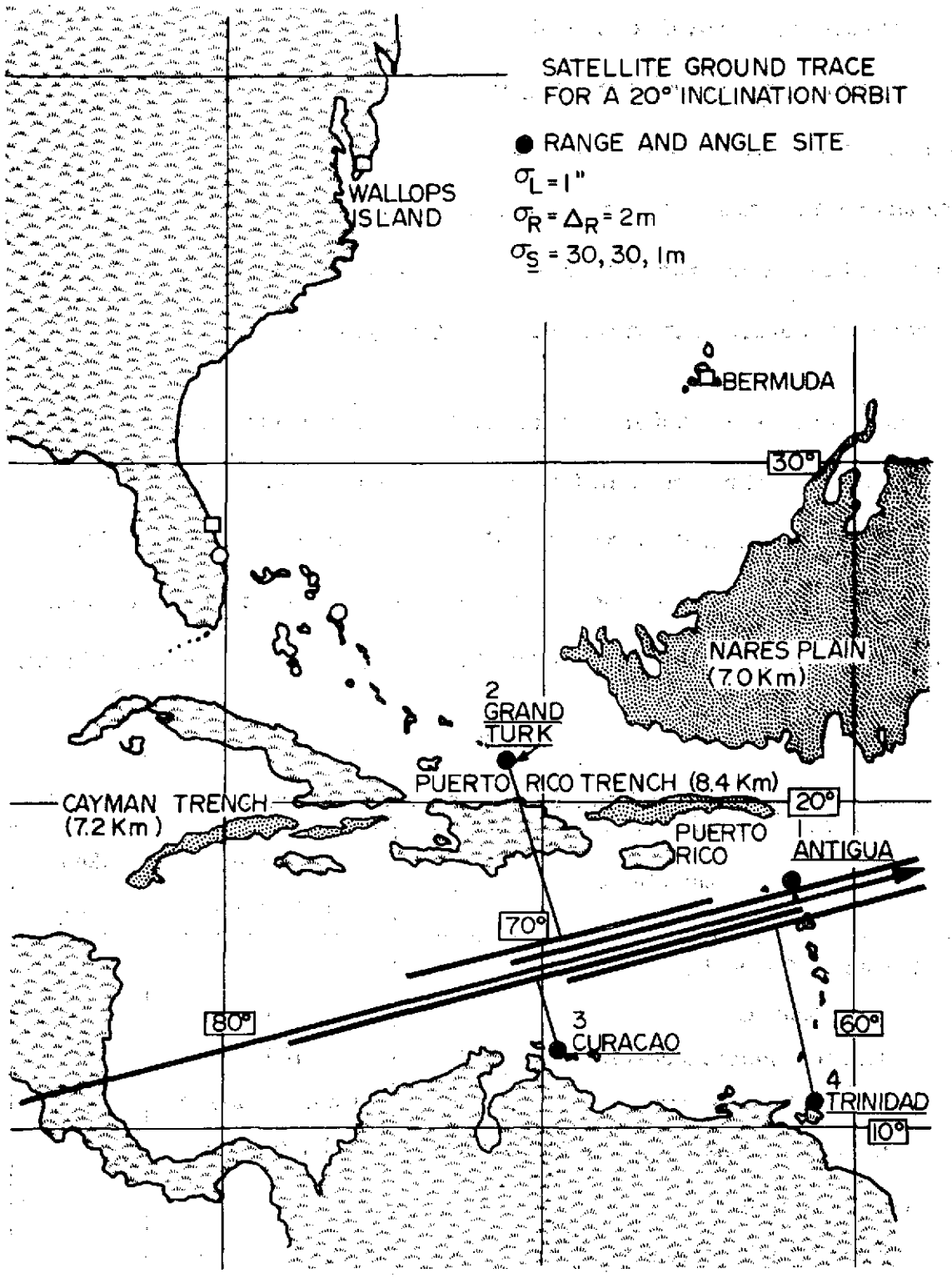
SATELLITE GROUND TRACE
FOR A 20° INCLINATION ORBIT
● RANGE AND ANGLE SITE
$\sigma_L = 1''$
$\sigma_R = \Delta_R = 2m$
$\sigma_{\underline{S}} = 30, 30, 1m$
WALLOPS ISLAND
BERMUDA
30°
NARES PLAIN (7.0 Km)
2 GRAND TURK
PUERTO RICO TRENCH (8.4 Km)
CAYMAN TRENCH (7.2 Km)
20°
PUERTO RICO
ANTIGUA
70°
80°
3 CURACAO
60°
4 TRINIDAD
10°

Figure 30

Results of an analysis of orbital altitude uncertainties determined by means of geometric error propagation using range and angle data from Antigua are seen in Figure 31. A reasonably conservative value of 2 meters is assumed for the laser range uncertainty and results for various values assumed for the angle uncertainties are indicated by the several curves. Accuracies of a second of arc should be achievable with cameras of the MOTS type, for example.

An analysis of a number of cases involving various combinations of lasers and cameras is summarized in Figure 32. Assumptions underlying these analyses are listed in Table XI. The other angle measure accuracies of 100" listed there were those assumed for the laser angles used in the analyses indicated by the open circles in Figure 32. In all cases, in addition to the altimeter

Table XI

GEOS-C Mission Altimeter Evaluation Analysis

Assumptions	A Priori Uncertainties	Noise rms
Recovered Quantities		
Range Measures	2 m	2 m
Altimeter Height Measures	100 m	10 m
Orbit – R&V Components	1 km, 1 km/sec	
Station Positions – E, N, V Components	30, 30, 1 m	
Other Quantities		
Camera Angle Measures		1"
Other Angle Measures		100"

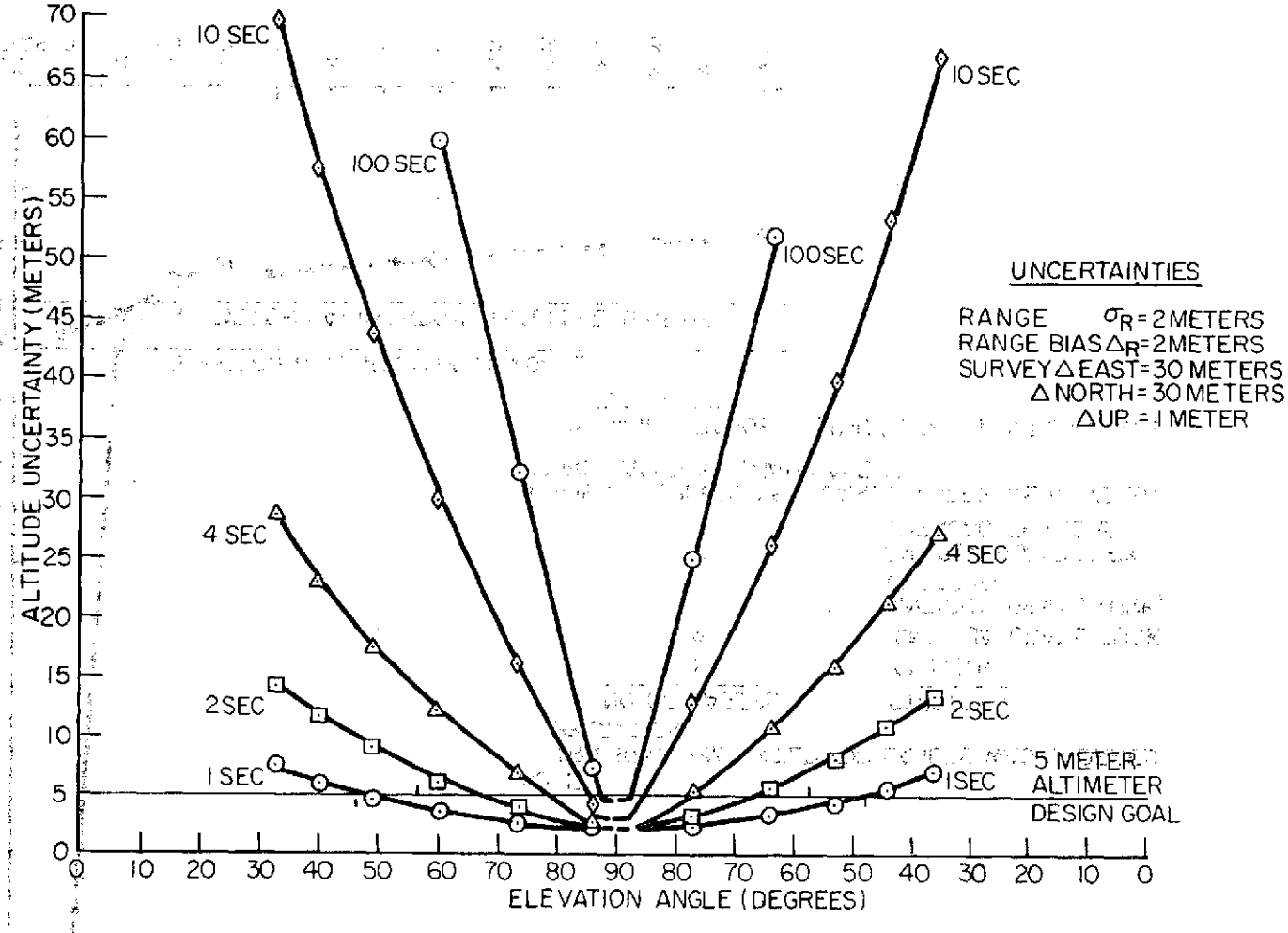
ALTITUDE UNCERTAINTY (METERS)
ELEVATION ANGLE (DEGREES)
10 SEC
100 SEC
4 SEC
2SEC
1 SEC
10SEC
100SEC
4 SEC
2 SEC
1SEC
5 METER ALTIMETER DESIGN GOAL
UNCERTAINTIES
RANGE σ_R = 2METERS
RANGE BIAS Δ_R = 2METERS
SURVEY Δ EAST = 30 METERS
Δ NORTH = 30 METERS
Δ UP = 1 METER

Figure 31

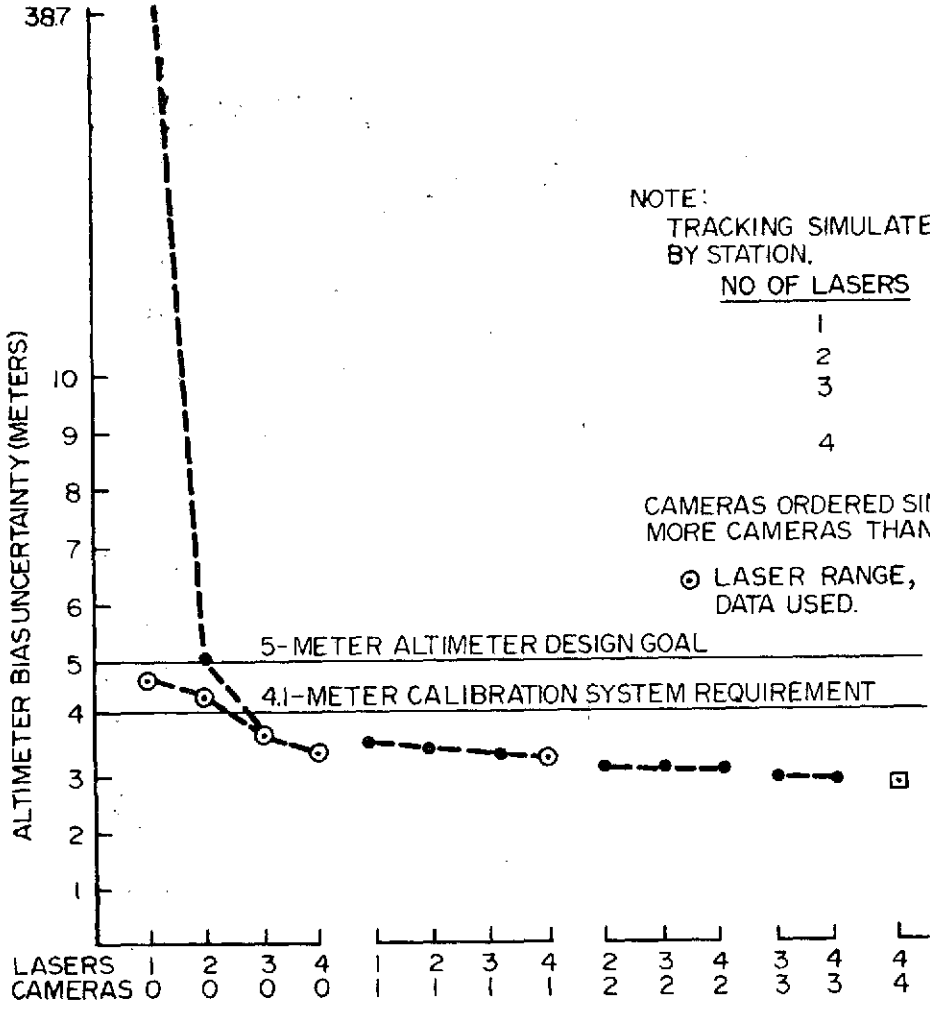
38.7
ALTIMETER BIAS UNCERTAINTY (METERS)
10
9
8
7
6
5
4
3
2
1
5-METER ALTIMETER DESIGN GOAL
4.1-METER CALIBRATION SYSTEM REQUIREMENT
LASERS 1 2 3 4 1 2 3 4 2 3 4 3 4 4
CAMERAS 0 0 0 0 1 1 1 1 2 2 2 3 3 4
NOTE:
TRACKING SIMULATED FOR LASERS WAS ORDERED BY STATION.
NO OF LASERS
STATIONS
1 ANTIGUA
2 ANTIGUA, GRAND TURK
3 ANTIGUA, GRAND TURK, CURACAO
4 ANTIGUA, GRAND TURK, CURACAO, TRINIDAD
CAMERAS ORDERED SIMILARLY. THERE WERE NEVER MORE CAMERAS THAN LASERS.
⊙ LASER RANGE, AZIMUTH & ELEVATION ANGLE DATA USED.

Figure 32

bias uncertainty, uncertainties in orbital, survey, and range measure parameters were also estimated. The triangle corresponds to a similar analysis of a three-laser-only case made for a much larger triangle based on stations at Antigua, Key West, and Panama. It resulted in a value of 4.1 meters, only slightly higher than that for the smaller triangle. As can be seen, a number of cases meet both the basic 4 meter requirement and the 3.5 meter figure obtained by allowing a couple of meters for uncertainties associated with the geoid.

Berbert and Loveless concluded that the 2-laser, 2-camera combination was probably the most cost effective in terms of the probabilities of obtaining reasonable amounts of data.

Tracking using lasers having ten centimeter accuracies can yield more accurate determinations of the orbit as has been pointed out by Vonbun (61). Results are indicated in Figure 33. The basic tracking system accuracy gives accuracies better than a meter. The limiting factor in this case would then appear to be the state of knowledge of the geoid which is thought to be on the order of a meter or two.

b. Long-Arc Tracking of GEOS-C

The surveys of the gravitational field over longer arcs will be greatly facilitated by the long-arc satellite-to-satellite tracking of GEOS-C which can be conducted through ATS-F. The accuracy capability of this tracking approach is indicated in Figure 34. In the case looked at here, accuracies of some four

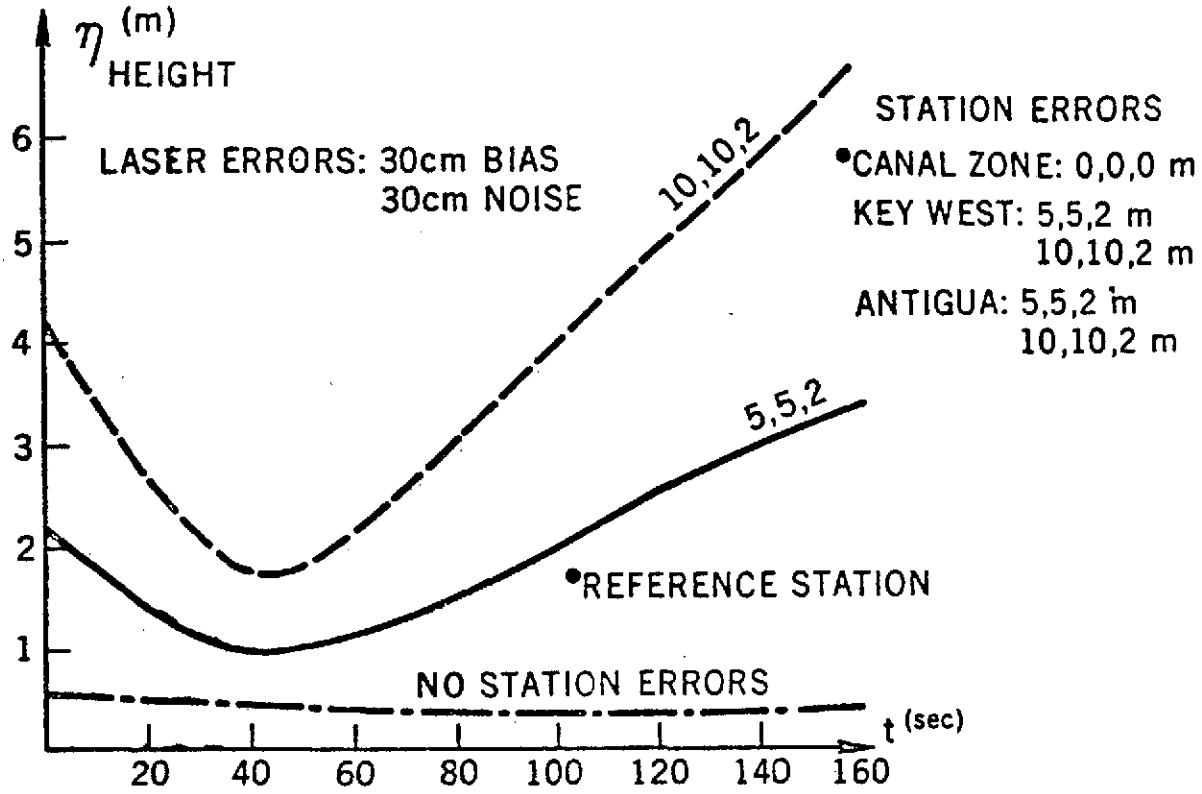

Figure 33. GEOS-C Height Errors Using Laser Tracking

meters or better persisted for almost three hours beyond the time interval shown in the Figure before the results deteriorated. Error analysis simulation results thus indicate that altitude accuracies in the three to four meter range can be achieved in this way. This is reasonably comparable to the current estimates of the accuracy of the world-wide geoid obtained from satellite orbit analysis (18). The latter has a spatial resolution of the order of 12°, however. Hence, altimeter and satellite-to-satellite tracking surveys even at the 6° resolution level will definitely provide new information. They will of course also provide the extremely valuable independent views which are so important.

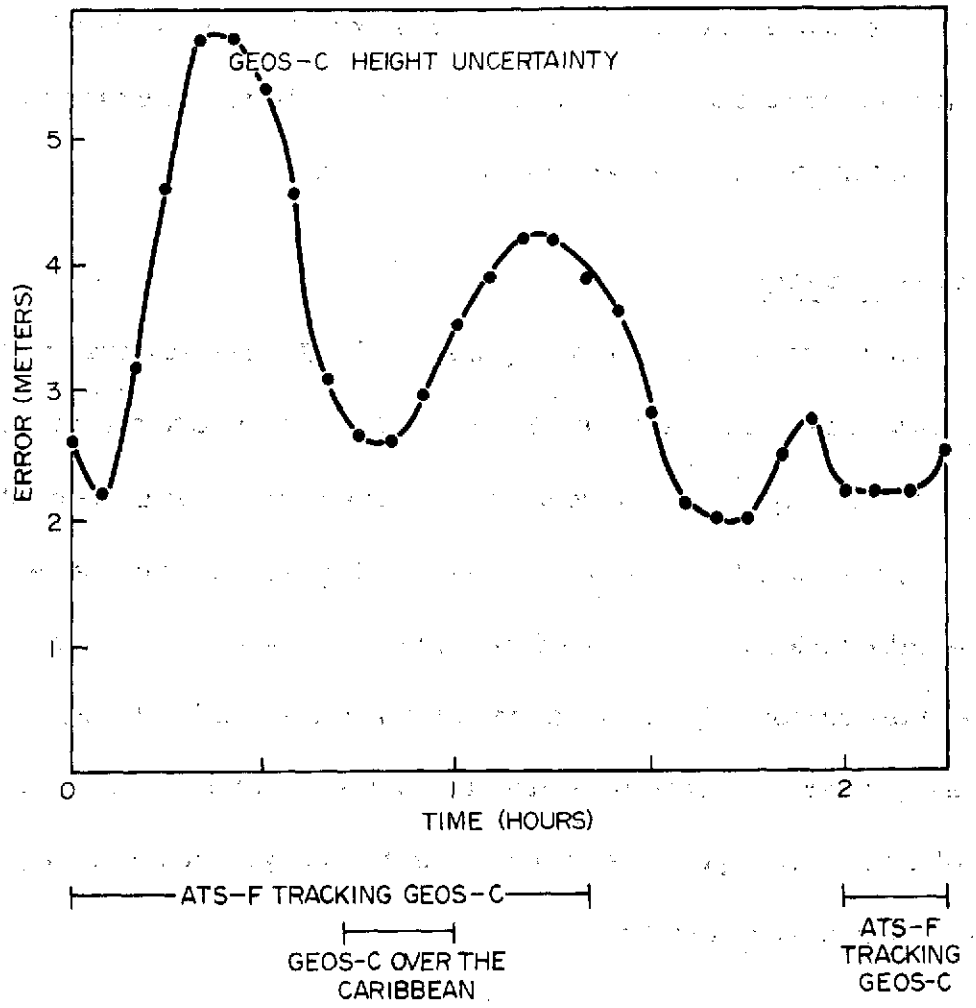

Figure 34

4. Ocean Surface Altitude Representation and Analysis Using Altimeter Data

The set of GEOS-C data will itself make possible a better representation of the effects indicated above. More than one kind of study holds promise. Tides can be analyzed on a global basis using all the altimeter data. Information about the geoid and the sea state can be sought everywhere. Current phenomena,

such as those associated with the Gulf Stream meanders, will be watched in certain regions of the oceans. Storm surges and Tsunamis will be looked at when and where they occur, in so far as this is feasible.

a. Gravimetry

Gravimetric investigations by means of a GEOS-C altimeter will include at least three kinds of studies. First, it will be possible to conduct an altimeter survey having a spatial resolution of about 6 degrees using the orbit ground track pattern which was worked out above in the discussion of the selection of a typical GEOS-C orbit. This will permit a direct inter-comparison with the results of the gravimetric investigation at the 6° resolution level which will be conducted by means of a satellite-to-satellite tracking system. A mutual validation of both the two approaches achieved in this way will increase the confidence in both types of results.

A similar altimeter gravimetric survey can be conducted at a finer resolution e.g., down to 1°. This can be thought of as the second type of experiment. This can also be conducted through the use of the GEOS-C orbit ground track pattern indicated earlier in the discussion of the GEOS-C orbit selection.

Thirdly, fine structure can be investigated in greater detail in regions of special interest such as those near the East and Gulf coasts of America. The interesting region in the neighborhood of the Puerto Rican Trench, for example, could be studied with the aid of the Caribbean facilities indicated in the calibration discussion.

Another possible region of this type will be discussed in a later section.

The results of these regional studies, will, it is expected, be correlated closely with the surface gravimetry data discussed above in Section III, C, i.

b. Tides

Zetler has pointed out, for example, that GEOS-C will, over its lifetime, provide data which can be used as the basis for a global tidal study (52).

A possible regional tidal study is discussed below in Section III, 4, C, i, B.

c. A Region for Earth and Ocean Dynamics Studies

As has been indicated above, surveys of certain phenomena such as the geoid and tides can be conducted on both global and regional bases. The following discussion deals with an area in which regional investigations of more than one type could be conducted fairly readily from a practical standpoint.

i. Ocean Dynamics

The Atlantic region off the coast of the Northeastern United States is of particular interest from the standpoint of the Gulf Stream meanders as was indicated in Figure 26 which is given by Hansen (57). These features have amplitudes on the order of a meter. Tidal variations in this same region, while not quite as large as those found elsewhere, are nevertheless of considerable size, i.e., of the order of a meter also. This is indicated in Figures 23 and 24, where the certain tidal components are seen (51, 53). This region is also a

reasonably attractive one from the standpoint of some of the practicalities of short-arc tracking. Good advantage could be taken of lasers which are usually available at Goddard, and possibly also at SAO.

An unusually useful system could be obtained by adding lasers at Bermuda and at a Bay of Fundy site chosen to be on the same meridian as Bermuda and as far north of Goddard as Goddard is north of Bermuda. This configuration is ideal for precision, short-arc tracking of GEOS-C. This can be seen readily from an inspection of Figure 35. Lasers having 10 centimeter accuracy capabilities will, when located at these sites, make it possible to determine the altitude of GEOS-C with relative accuracies of the order of a meter or better over a considerable portion of the region defined by the tracking sites at Goddard, Bermuda, and in the Bay of Fundy. A fourth laser at SAO would provide the important checks on the instrumental biases by providing the redundant information. It would also be most valuable in connection with reducing the impact of the cloud cover problem. As indicated above, this configuration has the important advantage of utilizing the fixed experimental lasers which are often available at Goddard and possibly also at SAO. This has the practical effect of bringing into action one or two additional lasers and hence increasing the total effective complement correspondingly.

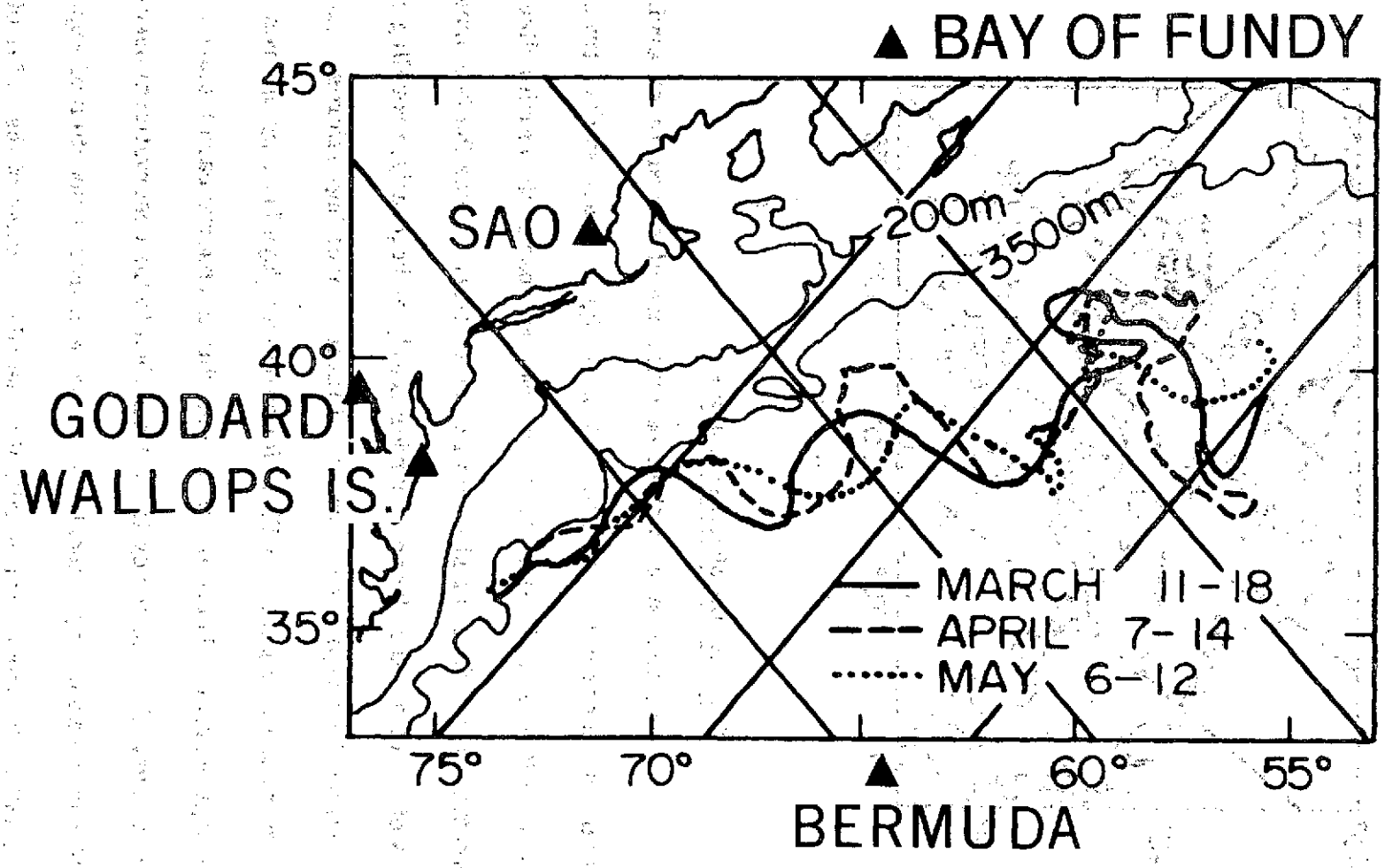
BAY OF FUNDY
45°
SAO
200m
3500m
40°
GODDARD
WALLOPS IS.
35°
MARCH 11-18
APRIL 7-14
MAY 6-12
75°
70°
60°
55°
BERMUDA

Figure 35

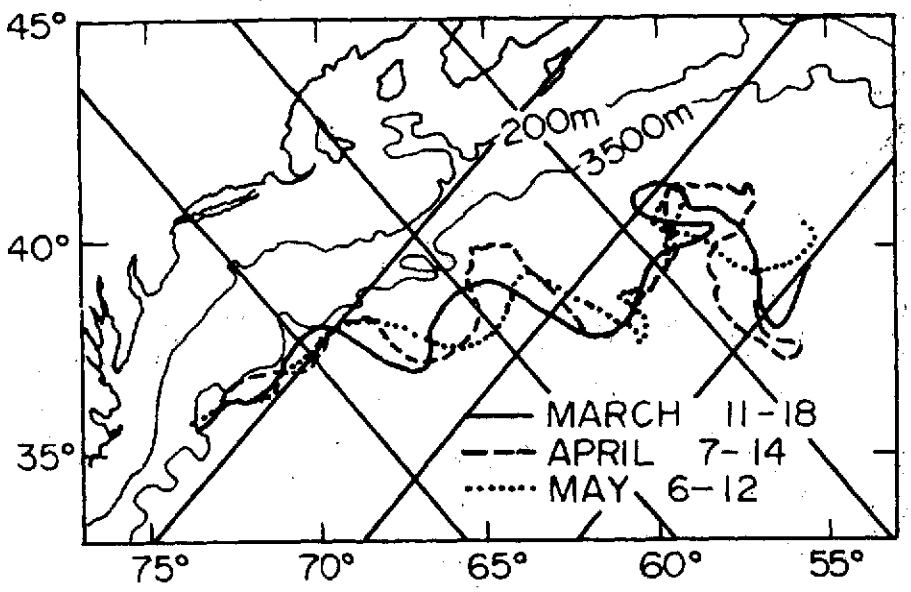

Figure 36

a. Gulf Stream Meander Studies

The altimeter tracking patterns are also good for observing the Gulf Stream meanders in this region. Shown in Figure 36 are surface tracks of the 65° orbit with 6.3° daily spacing which was obtained in the earlier discussion. It is seen that the northward and southward going tracks cross the two principal branches of a typical Gulf Stream meander nearly orthogonally, providing almost ideal geometry for studying the behavior of these interesting features. Each ground track seen in Figure 36 will be followed four days later by one removed just one degree from it, hence it will be possible to observe each feature once every four days. This frequency is well matched to the observational needs of a Gulf Stream meander experiment, as can be seen from inspection of Figures 27 and 36 (57). The mean wave length of a meander is often of the order of 300

kilometers, as was indicated above in the discussion associated with Figures 26 and 27. A typical meander moves a distance equal to its own wave length in about a couple of months. This interval might be thought of as a characteristic time constant which can be associated with the Gulf Stream meanders in this sense. Observations every four days are well suited for a Gulf Stream meander experiment. In fact observations every ten days or so would be most welcome, as Hansen has already pointed out (57). This also allows a margin for gaps in the observing program which might be due to such things as weather conditions or operational factors.

Similar studies of the Kuroshio current could be conducted by means of lasers similarly placed in Japan and nearby islands such as Iwo Jima, say.

β. Tidal Studies

Tidal studies can also be conducted in such regions by means of short-arc tracking. Once each day the GEOS-C altimeter satellite ground track passes through or very close to the Goddard-Bermuda-Bay of Fundy triangle as is indicated in Figures 36 and 37. At least one of the northbound tracks of the type seen in Figure 37, for example, would occur each day. These tracks are nearly orthogonal to the co-range lines of the semi-diurnal tide as can also be seen from Figure 37.

Southbound tracks, nearly parallel to the co-range lines, also occur daily in useful locations. The orbit selection worked out for GEOS-C in the above discussion

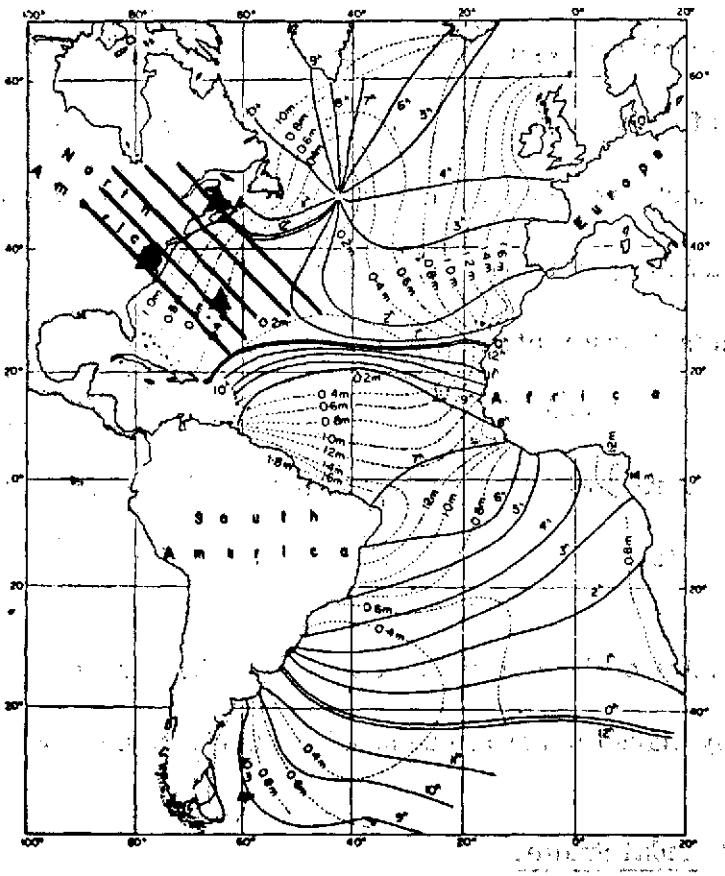

Figure 37. Theoretical tides of Atlantic Ocean. Full lines: co-tidal lines referred to moon-transition through meridian of Grw., dashed lines: co-range lines of the semi-diurnal tide M_2 in m (according to Hansen).

has the property of moving about 10.5 degrees each day relative to the moon. A complete cycle of the semi-diurnal lunar tide can thus be observed by GEOS-C about once every 17 days. The daily observations of GEOS-C in the Goddard-Bermuda-Bay of Fundy triangle would thus occur about 10.5° apart in this cycle, and hence provide ideal data for sampling this important tidal component. The interval between one day and the next can be thought of as corresponding to a bit over two-thirds of an hour in terms of the semi-diurnal cycle. Satellite-to-satellite

tracking may also be useful when combined with precision laser tracking in the Goddard-Bermuda-Bay of Fundy triangle in making observations in the neighborhood of the amphidromic point in the North Atlantic seen in Figures 23 and 24. Such a region could also be a good one in which to make the cross-over point checks which have been proposed by Stanley (59).

ii. Earth Dynamics

The Goddard-Bermuda-Bay of Fundy triangle also has other uses in connection with the Earth Dynamics side of the Earth and Ocean Dynamic Satellite Applications program (4).

α. Gravimetric Fine Structure

Fine structure in the gravity field should be deducible from observations made in this general area, but perhaps somewhat away from the immediate neighborhood of the Gulf Stream meanders.

β. Polar Motions and Earth's Rotational Rate Variations

The Bermuda-Bay of Fundy leg would be suitable for observing polar motion in the manner of the experiment conducted by Smith (62). The Goddard-Bermuda and Goddard-Bay of Fundy links taken together would also be useful for a companion experiment to observe the variations of the earth's rotational rate.

5. Altimeter Data Requirements

a. Gravitational Field Surveys

The altimeter survey conducted at the 6° resolution level would involve, as indicated above, portions of the equivalent of some 4 days of orbit tracks. Roughly speaking, some three days of "sea tracks" will occur, since the altimeter will be over land about a quarter of the time. Again, from the standpoint of 6 degree coverage, redundant information will be obtained near the maximum latitudes. As before, however, continuous coverage will be useful, at least to begin with. Accordingly, about 75 hours of altimeter observing will be required for the 6° survey, and some 450 hours for the one degree survey.

Such a set of observing programs will provide the basic data for gravimetric geodesy studies leading to the shape of the geoid, for example.

b. Tidal Analyses

These data will also be of real value in connection with a variety of oceanographic investigations including global tidal studies.

Additional types of observational data sets which would be useful for tidal studies can be considered in terms of the earlier discussion associated with Figures 23, 24, and 37, say, and the thinking about the GEOS-C orbit.

As pointed out there, the moon moves some 10.5 degrees per day relative to the GEOS-C orbit of the type contempated, and hence a cycle of the semi-diurnal lunar tidal component could be observed in about 17 days.

The durations of the northbound and southbound tracks of interest here would each be in the 10-minute range. Hence, about twenty-minutes a day of observing, or a total of some six hours in all would give data for a tidal study of this type. Repetitions of this type of study in different regions such as the Pacific and Indian Oceans and at different times would be important. In other situations, as many as five passes per day might prove to be useful. In such cases a total of about fifteen hours would be required for a study. Some half dozen such tidal experiments would involve approximately a hundred hours of altimeter observing time. Much of this might be in addition to the 75 or so hours for the 6° geoid survey. It would be included in the 450 hours or so needed for the 1° geodetic altimeter survey.

c. Gulf Stream Studies

The altimeter observation tracks described above in connection with the regional tidal study in the Western Atlantic would also serve as the basis for a study of the Gulf Stream meanders.

From the standpoint of the geoid study, the 6° and 1° resolution observations could be obtained anytime, in the sense that the gravity field is invariant over the lifetime, and to within the accuracy, of the GEOS-C experiment. Studies of tides and the Gulf Stream meanders require observations made in specific sequences as indicated in the above discussion. Hence, these should be given first priority in the scheduling except, of course, for observations of short-lived phenomena such as those associated with tsunamis and storm surges. Observations designed

to fill in the remaining regions required to complete the gravity surveys could then be scheduled so as to utilize the next increment of spacecraft capability.

d. Calibration

The altimeter calibration, which would precede studies discussed above, could also be conducted in the Goddard-Bermuda-Bay of Fundy traingle region in areas away from the meanders, near the coasts where ground truth is available. The calibration passes might in time be combined with the program to observe tides and meanders. Calibration and validation may thus involve only a small utilization of the GEOS-C resources relative to that which is envisioned for the scientific investigations, per se.

The Goddard-Bermuda-Bay of Fundy triangle can thus be used for altimeter calibration, Gulf Stream meander analyses, tidal studies, and polar motion and UT 1 observations.

IV. A SET OF SATELLITE-TO-SATELLITE TRACKING STUDIES

A. Introduction

It is presently planned to conduct satellite-to-satellite tracking experiments with GEOS-C and ATS-F, and with Nimbus-E and ATS-F. Consideration is also being given to equipping the Atmosphere Explorer and Small Astronomy Satellite-C (SAS-C) spacecraft with the capability for conducting satellite-to-satellite tracking operations with ATS-F. Such capabilities will be of value from the standpoing of the Gravimetric Geodesy Investigation and, in the case of the

Atmosphere Explorer spacecraft, for example, for operational reasons as well as is indicated in references 63 through 65. The operational considerations which are of special interest in connection with the AE program are discussed in reference 65. The present discussion will consider in more detail the aspects having to do with the gravitational field studies.

It is presently estimated that the ATS/GEOS and ATS/Nimbus tracking systems will have accuracies of about 2 meters in range and 0.035 centimeters per second in range rate. It will be assumed for the purposes of this discussion that the links between AE and ATS and SAS-C and ATS will have similar characteristics. The AE and SAS-C systems may turn out to be slightly less accurate, perhaps by a factor of two, than the Nimbus and GEOS systems for tracking through ATS. For this discussion however, it is convenient to assume that all these tracking systems will be similar, since this facilitates the understanding and comparison of the potential contributions of the different missions.

Estimated orbital parameters of the low altitude satellites involved are given in Table XII. In some cases these are not firm. GEOS-C for example may have an inclination in or near the 40 to 80 degree region. The values shown for the altitudes of the Atmosphere Explorers when they are in their nearly-circular, low-altitude orbits are used for planning purposes. Decisions will probably be made during each flight mission concerning the different height ranges which will actually be surveyed from the circular orbits in the 700 to

Table XII

Orbit Parameters Planned or Considered for Spacecraft Proposed for Satellite-to-Satellite Tracking Experiments

Spacecraft	Atltitude (kilometers)	Inclination (degrees)
Nimbus-E	1110, circular	100
GEOS-C	1000, circular	115
SAS-C	550, circular	3
AE-C	700, circular	65
	600, circular	65
	500, circular	65
	400, circular	65
	300, circular	65
	250, circular	65
	150, elliptical*	65
	120, elliptical*	65
AE-D	700, circular	100
	600, circular	100
	500, circular	100
	400, circular	100
	300, circular	100
	250, circular	100
	150, elliptical*	100
	120, elliptical*	100
AE-E	700, circular	20
	600, circular	20
	500, circular	20
	400, circular	20
	300, circular	20
	250, circular	20
	150, elliptical*	20
	120, elliptical*	20

*Perigee altitude,
Apogee altitude ~4000 km

250 kilometer altitude range toward the end of the spacecraft's active lifetime. Nevertheless certain kinds of observations can be made about an ensemble of orbits of the types seen in Table XII.

First, the array of different inclinations should be of real value. For example, range rate data will be taken over a given feature by satellites traversing at different angles in the orbits having different inclinations. It is anticipated that observable effects will frequently occur in two such distinct orbital paths when they pass over a given geographical region. Evidence of this type will be helpful in sorting out real physical effects from others which may be associated in some way with the analytical process. This point is discussed in reference 66, and in reference 40 in connection with Figure 11. It is seen that a variety of inclinations will be available ranging from within 3° of the equator to within 10° of the pole.

When satellites pass over regions having the same ground track but at different altitudes, it may be possible to learn more about the anomalous regions. For example, information may be obtained about the horizontal extent and/or the depth of the features involved. This point is discussed further in reference 40 in connection with Figure 11.

Two cases are of special interest here. GEOS-C may be in an orbit having an inclination of 115°, or 65° retrograde, which corresponds to the first Atmosphere Explorer at the inclination of 65°. These orbits will, in general, have ground

tracks over a given region which occur at different heights, and which are traversed in opposite directions. Nimbus-E and the second Atmosphere Explorer, AE-D, will both have the 100° inclination, but again will orbit at widely different altitudes.

The spatial resolutions obtainable with these spacecraft in the sense of the discussion of Section III, A, 2, associated with Figure 13 are indicated in Table XIII. Also shown here are the values for the resolution nodal longitude interval, λ, i.e., the spacing between equator crossings which corresponds to the spatial resolution, r, and the inclination, i, in the manner indicated in Section III, A, 2, i.e., $\lambda = r \csc i$. For a GEOS-C at a 40° inclination, but otherwise having the same characteristics as those indicated in the Table, the resolution nodal longitude interval would be about 8.9° for example.

Gravitational fields which have been derived recently on the basis of a combination of satellite data and gravimetry have spatial resolutions of 11° or so, or about 1200 kilometers near the equator. The geoids associated with them are considered to be reliable to about three meters. It is estimated that the information content of these fields which corresponds to spatial resolutions finer than about 18°, or about 2000 kilometers near the equator, is derived largely from the surface gravity data. (Cf. reference 18.)

It is seen from Table XIII that the satellite-to-satellite tracking experiments which are contemplated offer the prospect of improving the spatial resolution by factors in the range from about half to one order of magnitude.

Table XIII

Orbit and Gravimetric Geodesy Experiment Parameters for Spacecraft Proposed for Satellite-to-Satellite Tracking

Spacecraft	Altitude (kilometers)	Inclination (degrees)	Spatial Resolution (degrees)	Resolution Nodal Longitude Interval (degrees)
Nimbus-E	1110	100	6.2	6.3
GEOS-C	1000	115	5.7	6.3
SAS-C	550	3	4	90
AE-C	700	65	4.5	5.0
	600	65	4	4.5
	500	65	3.5	4.0
	400	65	3	3.4
	300	65	2.5	2.7
	250	65	2	2.4
	150*	65	1.5	1.6
	120*	65	1.2	1.4
AE-D	700	100	4.5	4.6
	600	100	4	4.2
	500	100	3.5	3.6
	400	100	3	3.1
	300	100	2.5	2.6
	250	100	2	2.2
	150*	100	1.5	1.5
	120*	100	1.2	1.3
AE-E	700	20	4.5	13.2
	600	20	4	12.0
	500	20	3.5	10.2
	400	20	3	9.0
	300	20	2.5	7.3
	250	20	2	6.3
	150*	20	1.5	4.3
	120*	20	1.2	3.6

*Perigee Altitude

The geoids associated with fields such as 1 through 5 in Table I are estimated to have accuracies on the order of 15 meters (69).

The latest solution in Table I, SAO 69 (II), when truncated at 8,8 does not represent an improvement over its predecessor, the SAO M-1 field. Except for resonant terms, the improvement found in the latest solution due to the satellite data is probably found chiefly in terms of the 9th and 10th degrees, some of which are poorly determined (18). The geoid associated with the general portion of the latest solution as it reflects satellite data is estimated to be somewhat better than fifteen meters but perhaps not greatly so.

Comparisons of the latest field with results obtained using recent gravimetric data indicate that uncertainties of five to seven meters are to be expected when the gravimetric data are relatively less dense and accurate (38). The characteristics of these results as they reflect satellite data, per se, are probably still less accurate.

It is estimated, thus, that the contribution of the satellite data to the most recent fields in Table I corresponds to a geoid accuracy on the order of ten meters, say, which in turn corresponds to some two and a half milligals. Accuracies comparable to this should be obtainable from 700 kilometer altitude orbits with the ATS satellite-to-satellite tracking system using 20-second integration times to achieve accuracies of the order of 0.15 to 0.2 millimeters per second. (Cf. Figure 13 and Reference 42.) A 30-second integration time

would give a tracking capability on the order of 0.1 millimeters per second which corresponds to an acceleration resolution capability of the order of 1.5 milligals in terms of sensing mean anomalies in squares about 5° on a side for a satellite at an altitude of 700 kilometers (42). In a sense, the ultimate range rate integration interval would correspond to the time required to pass over or traverse the square. A further improvement of perhaps a factor of two in tracking accuracy and the corresponding sensing capability might be achieved in this way. On this basis, the Atmosphere Explorer, in an orbit at about 250 kilometers altitude, would have an acceleration resolution capability of the order of half a milligal. This may be somewhat optimistic, hence it will be assumed, more conservatively, that the acceleration resolution capability of the Atmosphere Explorer in a 250 kilometer orbit will be on the order of a milligal. The acceleration resolution capability of GEOS-C and

Nimbus-E is estimated to be on the order of a couple of milligals, and the acceleration resolution of SAS-C is estimated to be on the order of a milligal and a half. In making these various estimates, it was assumed in accordance with Schwarz's finding that the sensitivities vary roughly as the reciprocal of the altitude in this general range (42, 70).

The estimated acceleration resolutions to be derivable from the satellite-to-satellite tracking results appear to be a little better than those we have now from satellites; however, the differences between the two kinds of estimates may

be no more than their uncertainties. Improvements of the order of perhaps a factor of two in acceleration resolution will be looked for in some cases.

Certain additional features of interest which are associated with these different contemplated experiments are indicated in the following discussion.

B. Nimbus-E

The Nimbus-E/ATS-F experiment is expected to be the first of the satellite-to-satellite tracking experiments. As was indicated in the above discussion, it will provide us with an improvement of nearly a factor of three in spatial resolution. It will also, of course, give us our first experience with this new type of data and technique.

The 6.6 bi-daily nodal longitude interval which is indicated in Table XIV implies that some 27 orbital arcs of interest will be trackable from ATS-F in a given position. There is both a northbound and a southbound pass associated with each interval hence some 54 arcs will be of interest. The total tracking interval will be approximately 54 hours. ATS will at first be at 94° west longitude and later at 35° east longitude. A second survey centered at the eastern longitude will involve another 54 arcs and another fifty-four hours. Some fifteen hours will involve overlapping coverage which should be useful for correlative and corroborative purposes. In addition, as ATS moves from one location to another, satellite-to-satellite tracking could provide additional data having different geometrical characteristics. In all some three such surveys, centered at about 94° west, 35° east, and 30° west, would be very valuable.

Table XIV

Gravimetric Geodesy Experiment Parameters and Observation Requirements for Certain Spacecraft Proposed for Satellite-to-Satellite Tracking

Spacecraft	Altitude (kilometers)	Resolution Nodal Longitude Interval (Degrees)	Daily or Bidaily Nodal Longitude Interval (Degrees)	Number of Arcs Per Survey	Number of Hours Per Survey
Nimbus-E	1110	6.3	6.6*	54	54
GEOS-C	1000	6.3	6.3	57	56
SAS-C	550	90	–	4	3

*Bidaily

C. GEOS-C

The GEOS-C satellite orbit is presently envisioned to be somewhat lower than the NIMBUS-E orbit. This will offer a corresponding increase in resolution. Also the GEOS-C orbit will not be subject to perturbations by control jets. In addition, the orbit of GEOS-C will be known much more accurately, independently of the satellite-to-satellite tracking, through the use of the very accurate geodetic tracking systems which it will employ. Hence, it is the ideal satellite on which to really evaluate the satellite-to-satellite tracking system as was pointed out in reference 67 in which this experiment was first proposed. The GEOS-C satellite will, in addition, as was pointed out above, also provide data at another inclination. Observational requirements worked out along the lines indicated in the discussion of the NIMBUS-E case are indicated in Table XIV.

D. SAS-C

The SAS-C spacecraft, orbiting at a relatively low altitude, will afford a still further increase in spatial resolution and a gain of nearly a factor of two in acceleration resolution. SAS-C will also add data at still another inclination. Again, observational requirements are listed in Table XIV.

E. The Atmosphere Explorers

The Atmosphere Explorers will provide a marked increase in the capabilities for both spatial resolution and acceleration resolution. They will also, as was pointed above, provide data at three inclinations, and at a number of heights for each of these inclinations. This will enhance considerably the value of this phase of the Gravimetric Geodesy Investigation.

Gravimetric Geodesy Investigations which can be performed with Atmosphere Explorer by means of satellite-to-satellite tracking are of two types, those associated with the elliptic orbits and those associated with the circular orbits. Present plans call for an elliptic orbit for AE-C having an inclination of 65°, an apogee of about 4000 km., and a perigee height which will usually be about 150 km, and which will be lowered to about 120 km for one day in each two weeks. The circular orbits will be at several heights ranging from about 250 to 700 km.

For the elliptic case the orbit having a perigee of about 150 km will be in existence long enough to permit a survey to be made. The altitude of about 150

km corresponds to a spatial resolution of 1.5 degrees in the sense of the discussion of Section III, A, 1, which is associated with Figure 13. The planned orbit is close to one which will have a daily nodal separation of 1.6 degrees. This will be the appropriate spacing for the case in which the perigee is near the equator, which is one of the possibilities now under consideration. If the perigee is far from the equator, the survey can be completed with a correspondingly larger nodal spacing and with correspondingly fewer passes than is indicated here.

A slight increase in the period of the orbit, of the order of a minute, and a corresponding increase in apogee height, of the order of a 100 km, will give a daily nodal spacing of 1.6 degrees. This orbit, then, will permit the making of a survey which would provide the coverage to correspond to the lowest altitude reached by the AE-C spacecraft in such a case. The altitude region between 150 and 1110 km would be of interest. This would permit correlation of results with those obtained from all the satellites to be tracked from ATS, i.e., Nimbus-E, GEOS-C, and SAS-C. The Atmosphere Explorer will be below 1110 km over a true anomaly range of about 142°, or for about 34 minutes per revolution. Some 100 arcs under ATS when it is at a given location would suffice to complete a survey at the 1.5 degree resolution level. Roughly speaking, one pass every other day during the eight months or so when AE-C is in the elliptical orbit would be sufficient. An additional eighty passes would complete the survey if ATS would move between 94° west and 35° east during this period. Thus a total of

some 180 passes, or less than one pass per day on the average, would suffice for the entire longitude history of ATS-F. The corresponding tracking time requirements are about 57 hours for the 100 passes and 105 hours for the 180 passes.

If the perigee is at the equator, each arc which is of interest can be observed from ATS during one continuous interval. If the perigee is at the pole, the arcs of interest would be observed in two equal portions, when the ATS is on either side of the AE-C orbit. When perigee occurs in an intermediate position the arcs of interest would be observed from ATS in two unequal time intervals occurring when ATS is on either side of the AE orbit. The total observing time would be about the same for all these cases, i.e., about 105 hours.

The dipping down of the perigee to 120 km altitude provides a spatial resolution that is even finer, i.e., about 1.2°. In view of the limited time during which the perigee will be at these low altitudes, however, a complete survey would probably not be practical. Nevertheless the observation of portions of the orbit at this height from ATS at different longitudes would be of great interest.

The circular orbits planned for the AE missions would also be of great value from the gravimetric geodesy standpoint. There is interest in matching the nodal spacing at the equator to the spatial resolution capability associated with the altitude. It is seen from Table XV that the desired resolution nodal longitude intervals do not correspond too well with the daily or bidaily nodal

Table XV

Gravimetric Geodesy Experiment Parameters for Certain Possible Atmosphere Explorer-C Orbits

Altitude (kilometers)	Resolution Nodal Longitude Interval (Degrees)	Daily or Bidaily Nodal Longitude Interval (Degrees)
700	5.0	1.2*
600	4.5	6.9
500	4.0	0.8
400	3.4	2.9*
300	2.7	6.9
250	2.4	2.9

*Bidaily

longitude intervals associated with the orbits at the nominal altitudes at the 100 kilometer intervals.

The nodal spacing could be matched to the desired spacings more closely by modifying somewhat the periods and altitudes listed in Table XV. The orbital altitude parameters in or near the range from 250 to 700 km which are close to those considered for the Atmosphere Explorer C and which would also yield the nodal separations that can form the basis for good gravimetric geodesy experiments are indicated in Table XVI. It is seen that only relatively small changes from the nominal orbits would suffice in most cases.

C-2

Table XVI

Experiment Parameters and Observation Requirements for Certain Possible Atmosphere Explorer-C Orbits Which Would be Valuable for the Gravimetric Geodesy Investigation

Altitude (kilometers)	Resolution Nodal Longitude Interval (degrees)	Daily or Bidaily Nodal Longitude Interval (degrees)	Number of Arcs per Survey	Number of Hours per Survey	Number of Arcs per 45° Survey	Number of Hours per 45° Survey
725	5.1	5.1*	63	45	35	17
570	4.4	4.4	73	50	41	19
460	3.7	3.7	87	58	49	22
405	3.4	3.4*	94	62	53	23
240	2.3	2.3	139	88	78	33
150-4100	1.6	1.6	100	57		

*Bidaily

The approximate values shown in Table XVI are suggested for illustrative purposes. It is anticipated that further study of the matter of orbit selection from the standpoint of the atmospheric research requirements and the gravimetric geodesy criteria could reveal orbit parameters which would meet the atmospheric experimenters needs and at the same time make it possible to conduct valuable gravimetric geodesy experiments.

It is seen from Table XVI that on the order of 60 to 140 passes of nearly half an orbit in length would be of interest at the heights shown there. The AE

satellite will spend only some 10 or 30 days at each of these altitudes, however. Thus, from two to fourteen passes per day would be required, which may be beyond the resources available. In such a case, a more limited survey could be attempted.

A useful survey could be conducted over the region lying within about 45° of the sub-ATS region. This would involve only a much smaller number of arcs, and each one would not be nearly so long as in the case of the complete survey. Hence only a fraction of the observing time would be required for such a limited survey. Such a survey would correspond reasonably well to the type of experiment which was conducted in connection with the discovery of the lunar mascons.

The satellite-to-satellite tracking system for use between AE and ATS will have an accuracy of about 0.035 cm per second for a ten second integration interval. This corresponds to an acceleration of about 3.5 milligals. It is planned that the accelerometer to be used in connection with the atmospheric density experiments will operate over two resolution ranges while the experiment is in progress. These extend, respectively, from 5×10^{-4} to 10^{-6} g, and from 10^{-5} to 2×10^{-8} g. It appears, then, that the accelerometer resolution will be adequate for the needs of the Gravimetric Geodesy Investigation.

Some of the parameters of geodetic interest associated with the spacecraft discussed here are summarized in Table XVII.

Table XVII

Parameters of the Geodetic Interest Associated With the Spacecraft

Spacecraft	Inclination (degrees)	Altitude (kilometers)	Approximate Spatial Resolution (Degrees)	Order of Acceleration Resolution (milligals)
Existing set of Spacecraft			18	2.5
Nimbus-E	100	1111	6.2	2
GEOS-C	115	1000	5.7	2
AE-C	65	725	4.6	1.5
SAS-C	3	550	4	1.5
AE-C	65	240	2	1

V. MANAGEMENT CONSIDERATIONS

It is expected that a general solution for the geopotential, including the ISAGEX data, can be obtained by the time the GEOS-C data become available. It is anticipated that the first analysis of the GEOS-C data will be achieved within a year after they are received. The analyses will continue correspondingly as additional data are provided. Reports of results of the analyses and solutions will include new representations of the Earth's gravitational field.

It is a pleasure to acknowledge many helpful discussions with a number of individuals at Goddard and other institutions including many in connection with satellite geodesy whose works are cited in the references and a number in connection with oceanographic studies including Drs. W. S. Von Arx, C. Bowen, and K. Hasselmann of the Woods Hole Oceanographic Institution, Dr. K. Bryan of the

NOAA Laboratory, Princeton, Drs. J. R. Apel, B. D. Zetler and D. V. Hansen of the NOAA Atlantic Oceanographic and Meteorological Laboratories, Drs. W. H. Munk and M. C. Hendershott of the Scripps Institution of Oceanography, La Jolla, California, Dr. W. J. Pierson, Jr. of the New York University, Dr. W. Sturges of the University of Rhode Island, Dr. M. Talwani of the Lamont-Doherty Geological Observatory, and Dr. B. Yaplee of the Naval Research Laboratory.

REFERENCES

1. GEOS-A Mission Plan, National Geodetic Satellite Program Office, NASA, September 16, 1965.
2. Project Plan For the Geodetic Earth Orbiting Satellite (GEOS-C), Review Draft, NASA Wallops Station, September, 1971.
3. NASA, "The Terrestrial Environment: Solid Earth and Ocean Physics" Prepared by MIT for NASA, ERC, April, 1970.
4. "Earth and Ocean Dynamics Satellite Applications Program," NASA, Washington, D.C., April 1, 1971 (Preliminary Issue).
5. Anderle, R. G., "Observations of Resonance Effects on Satellite Orbits Arising from the Thirteenth and Fourteenth-order Tesseral Gravitational Coefficients," Journal of Geophysical Research, Volume 70, No. 10, May, 1965.
6. Guier, W. H., and Newton, R. R., "The Earth's Gravitational Field as Deduced from the Doppler Tracking of Five Satellites" Journal of Geophysical Research, Volume 70, No. 18, September 1965.
7. Lindquist, C. A., and Veis, G., "Geodetic Parameters for a 1966 Smithsonian Institution Standard Earth," Smithsonian Astrophysical Observatory Special Report No. 200, 1966.
8. Kaula, W. M., Journal of Geophysical Research, Volume 71, No. 22, pages 5303-5314, 1966.

9. Rapp, R. H., "The Geopotential to (14,14) from a Combination of Satellite and Gravimetric Data," presented at the XIV General Assembly International Union of Geodesy and Geophysics, International Association of Geodesy, Lucerne, Switzerland, October 1967.

10. Köhnlein, W., "The Earth's Gravitational Field as Derived from a Combination of Satellite Data with Gravity Anomalies," Smithsonian Astrophysical Observatory Special Report No. 264, pages 57-72, December 1967.

11. Kaula, W. M., Publication No. 656, Institute of Geophysics and Planetary Physics, University of California, Los Angeles, December 1967.

12. Rapp, R. H., "A Global 5° × 5° Anomaly Field," Presented at the 49th Annual American Geophysical Union Meeting, April 1968.

13. Gaposchkin, E. M., "Improved Values for the Tesseral Harmonics of the Geopotential and Station Coordinates," presented at the XII COSPAR Meeting, Prague, May 1969, Smithsonian Astrophysical Observatory.

14. Gaposchkin, E. M., Private Communication, U.S. Gov't Memorandum, July 22, 1969.

15. Gaposchkin, E. M., Private Communication, U.S. Gov't Memorandum, October 7, 1969.

16. Gaposchkin, E. M. and Lambeck, K., "New Geodetic Parameters for a Standard Earth," presented at the Fall Meeting of the American Geophysical Union, San Francisco, California, December 1969.

17. Murphy, James P., Marsh, J. G., "Derivation and Tests of the Goddard Combined Geopotential Field (GSFC 1.70-C), "Goddard Space Flight Center Report No. X-552-70-104, January 1970.

18. Gaposchkin, E. M., and Lambeck, K., "1969 Smithsonian Standard Earth (II)," SAO Special Report 315, May 18, 1970.

19. Wagner, C. A., "Resonant Gravity Harmonics from 3-1/2 Years of Tracking Data on Three 24-Hour Satellites," Goddard Space Flight Center Report No. X-643-67-535, November 1967.

20. Gaposchkin, E. M., and Veis, G., "Comparisons of Observing Systems and the Results Obtained from Them," Presented at the COSPAR meeting, London, July 1967.

21. Murphy, J., and Victor, E. L., "A Determination of the Second and Fourth Order Sectorial Harmonics in the Geopotential From the Motion of 12-Hr. Satellites," Planetary and Space Science Vol. 16, pp. 195-204, 1968.

22. Yionoulis, S. M., "Improved Coefficients of the Thirteenth-Order Harmonics of the Geopotential Derived from Satellite Doppler Data at Three Different Orbital Inclinations," Johns Hopkins/Applied Physics Laboratory Report TG-1003, May 1968.

23. Wagner, C. A., "Determination of Low-Order Resonant Gravity Harmonics from the Drift of Two Russian 12-Hour Satellites," Journal of Geophysical Research, Vol. 73, No. 14, July, 1968.

24. Murphy, J. P., Cole, I. J., "Gravity Harmonics from a Resonant Two-Hour Satellite," GSFC X-552-68-493, December 1968.

25. Wagner, C. A., "Combined Solution for Low Degree Longitude Harmonics of Gravity from 12- and 24-Hour Satellites," Journal of Geophysical Research, Vol. 73, No. 24, December 1968.

26. Douglas, B. C., Marsh, J. G., "GEOS-II and 13th Order Terms of the Geopotential," Celestial Mechanics 1 (1970) 479-490, August, 1969.

27. Wagner, C. A., Fisher, E. R., "Geopotential Coefficient Recovery from Very Long Arcs of Resonant Orbits," GSFC X-552-69-498, November 1969.

28. Siry, Joseph W., "Geodetic and Orbital Research at the NASA Goddard Space Flight Center," Presented at the Conference on Scientific Research Using Observations of Artificial Satellites of the Earth, Bucharest June 1970.

29. Siry, Joseph W., "Astronomic and Geodynamic Parameters," Goddard Space Flight Center Report No. X-550-70-481, November 1970.

30. Velez, C. E., Brodsky, G. P., "Geostar I, A Geopotential and Station Position Recovery System," GSFC Report No. X-553-69-544, November 1969.

31. Murphy, J. P., Felsentreger, T. L., "Analysis of Lunar and Solar Effects on the Motion of Close Earth Satellites," NASA TN D-3559, August 1966.

32. Brouwer, D., "Solution of the Problem of Artificial Satellite Theory Without Drag," A. J., 64, 378-397, 1959.

33. Siry, J. W., Murphy, J. P., and Cole, I. J., "The Goddard General Orbit Determination System" Goddard Space Flight Center Report No. X-550-68-218, May 1968.

34. Lerch, F. J., Marsh, J. G., D'Aria, M. D., Brooks, R. L., "GEOS-I Tracking Station Positions on the SAO Standard Earth (C-5), "NASA TN D-5034, June 1969.

35. Berbert, J. H., Loveless, F., Lynn, J. J., "GEOS Station Position Solution Comparisons, "Trans. Am. Geophys. Un. 50, 602, 1969.

36. Marsh, J. G., Douglas, B. C., and Klosko, S. M., "A Unified Set of Tracking Station Coordinates from Geodetic Satellite Results," Goddard Space Flight Center Report No. X-552-70-479, November 1970.

37. Marsh, J. G., Douglas, B. C., and Klosko, S. M., "A Unified Set of Tracking Station Coordinates Derived From Geodetic Satellite Tracking Data," GSFC Report No. X-553-71-370, July 1971.

38. Marsh, J. G., Private Communication.

39. Felsentreger, T. L., Murphy, J. P., Ryan, J. W., Salter, L. M., "Lunar Gravity Fields Determined from Apollo 8 Tracking Data, NASA TMS 63666, July 1969.

40. Murphy, J. P., Siry, J. W., "Lunar Mascon Evidence from Apollo Orbits," Planetary and Space Science, Vol. 18, pp. 1137 to 1141, 1970.

41. Vonbun, F. O., "The ATS-F/Nimbus-E Tracking Experiment," Presented at the 48th IAU Symposium, May 9-15, 1971, Morioka, Japan.

42. Schwarz, Charles R., "Gravity Field Refinement by Satellite to Satellite Doppler Tracking," Department of Geodetic Science Report No. 147, Ohio State University Research Foundation, December 1970.

43. Siry, Joseph W., "Satellite Altitude Determination Uncertainties," Presented at the NOAA, NASA, NAVY Sea Surface Topography Conference, Key Biscayne, Florida, October 6, 1971.

44. Von Arx, W. S. (1966) Level-Surface profiles across the Puerto Rico Trench, SCIENCE, 154 (3757), 1651-1654.

45. Talwani, M., "The Ocean Geoid," Presented at the NOAA, NASA, NAVY Sea Surface Topography Conference, Key Biscayne, Florida, October 6, 1971.

46. Uotila, U. A., Rapp, R. H., and Karki, P. A., "The Collection, Evaluation and Reduction of Gravity Data," Report No. 78, Department of Geodetic Science, The Ohio State University Research Foundation, Columbus, Ohio, October 1966.

47. Rapp, R. H., "Accuracy of Potential Coefficients Obtained From Present and Future Gravity Data," Presented at the Symposium on Geodetic Uses of Artificial Satellites, Washington, D.C., April, 1971.

48. Strange, W. E., Vincent, S. F., Berry, R. H., and Marsh, J. G., "A Detailed Gravimetric Geoid For the United States," Goddard Space Flight Center Report No. X-552-71-219, June 1971.

49. Strange, W. E., Private Communication.

50. Talwani, M., Private Communication.

51. Hendershott, Myrl, and Munk, Walter, "Tides," Annual Review of Fluid Mechanics, Vol. 2, pp. 205-224, 1970.

52. Zetler, B., and Maul, G. A., "Precision Requirements for a Spacecraft Tide Program," Journal of Geophysical Research," 76, 6601-6605, 1971.

53. Hansen, W., "Die halbtagigen Gezeiten im Nordatlantischen Ozean, Dtsch. Hydr. Z. 2, 44-51 (1949).

54. Hendershott, Myrl, Private Communication.

55. Stommel, Henry, "Summary Charts of the Mean Dynamic Topography and Current Field at the Surface of the Ocean, and Related Functions of the Mean Wind-Stress," Studies on Oceanography, 53-58, 1964.

56. Bryan, K., Private Communication.

57. Hansen, Donald V., "Gulf Stream Meanders Between Cape Hatteras and the Grand Banks," Deep Sea Research, 17, 495-511, 1970.

58. Pierson, Willard J., Jr., and Mehr, Emanuel, "The Effects of Wind Waves and Swell on the Ranging Accuracy of a Radar Altimeter," New York University Report, January, 1970.

59. Stanley, H. Ray, Private Communication.

60. Berbert, John H., and Loveless, Fred M., "A Satellite Altimeter Bias Recovery Simulation," GSFC X-550-71-224, May 1971.

61. Vonbun, F. O., "Satellite-to-Satellite Tracking and It's Contribution to Spacecraft Altimetry," Presented at the NOAA, NASA, NAVY Sea Surface Topography Conference, Key Biscayne, Florida, October 6, 1971.

62. Smith, D. E., Kolenkiewicz, R., and Dunn, P. J., "Geodetic Studies By Laser Ranging to Satellites," Presented at the Third International Symposium on the Use of Artificial Satellites For Geodesy," Washington, D.C., April 1971.

63. Siry, J. W., "Atmosphere Explorer Design Review," Memorandum, April 3, 1970.

64. Siry, J. W., "An Atmosphere Explorer/ATS Satellite-to-Satellite Tracking, Orbit Determination and Data Transmission Capability" Memorandum to D. W. Grimes, February 24, 1971.

65. Siry, J. W., "Earth and Ocean Dynamics Satellite Applications Program: Satellite-to-Satellite Tracking Between Atmosphere Explorer and ATS, and Between SAS and ATS," Memorandum to Chairman, Earth Physics Working Group, June 2, 1971.

66. Muller, P. M., and Sjogren, W. L., "Mascons: Lunar Mass Concentrations," Science, 161, 680-784 (1968).

67. Siry, J. W., "Proposed Earth Physics and Geodesy Programs Including an ATS-GEOS Tracking and Orbit Determination Experiment" letter to NASA Headquarters, J. Naugle and J. Rosenberg with enclosure, August 27, 1969.

68. Felsentreger, T. L., Grenchik, T. J., and Schmid, P. E., "Geodetic Earth Orbiting Satellite (GEOS-C) - Applications Technology Satellite (ATS-F) Tracking Experiment," GSFC X-552-70-96, March 1970.

69. Kaula, W. M., "The Appropriate Representation of the Gravity Field for Satellite Geodesy," Proceedings of the IV Symposium on Mathematical Geodesy, Trieste, 57-65, 1969.

70. Schwarz, C., Private Communication.